THE NEURAL CORRELATES OF SOCIAL AND NON-SOCIAL DECISION-MAKING IN RESOLVING COMPLEX, DYNAMIC UNCERTAINTY

A Dissertation
Submitted to
the Temple University Graduate Board

In Partial Fulfillment
of the Requirements for the Degree
DOCTOR OF PHILOSOPHY

---

by
William John Mitchell III
December 2025

Examining Committee Members:

Chelsea Helion, Advisory Chair, Social Psychology
Jason Chein, Social Psychology
David Smith, Cognition and Neuroscience
Vishnu P. Murty, Cognition and Neuroscience
Thomas Olino, External Reader, Clinical Psychology

ABSTRACT

Understanding how people form appraisals under uncertainty is a foundational challenge for social cognition research. Naturalistic stimuli are a powerful tool for modeling these processes, but the cognitive and neural dynamics that govern real-time appraisal during complex narratives remain underexplored. Across three studies, this dissertation investigated how individuals dynamically appraise social and non-social ambiguity using a 45-minute episode of a murder mystery drama. In the first fMRI study, participants continuously rated their certainty regarding a primary character's guilt. Neural synchrony during this appraisal task was examined via inter-subject correlation and sliding window approaches, revealing temporally dynamic, content-sensitive neural alignment in social-cognitive networks. The second study extended this design behaviorally, examining the structure and variability of hypothesis generation across individuals. The third study manipulated appraisals directly, instructing participants to assess the informativeness of scenes in relation to a guilt hypothesis. Integrating these findings, the dissertation demonstrates that stimulus complexity and interpretive framing jointly modulate appraisal synchrony, and that these processes are supported by distributed regions in the default mode, salience, and attentional networks. These findings advance our understanding of how people resolve social ambiguity in real time and highlight the value of continuous self-report and dynamic brain-behavior alignment in naturalistic settings. Implications for social inference and real-world decision-making are discussed.

For my father, who never sat in the shade of the trees he planted,

and for my daughter, that she will one day rest beneath them.

ACKNOWLEDGMENTS

First, I am deeply grateful to my dissertation committee for their patience and flexibility in waiting on this document. It turns out dissertating with a gassy newborn is hard. To Chelsea: thank you for taking a chance on me. You gave me both the opportunity to watch the lab from its inception and the privilege of growing alongside it. If not for that decision, I would never know Joy, Ginny, Helen, Melanie, Emma, Isabel, and all the incredible people who have shaped me in ways I could never forget. I could not have asked for a better mentor than Chelsea. Every skill I've developed, every moment of pride I experienced stems from your guidance. Thank you for being unreasonably accommodating - my unfruitful fixations, scattered focus, or personal interests that did not always align with the lab's forward motion - you always gave me the space to pursue what I thought was important. To Deepu: thank you for challenging me and for showing me what it means to pursue research with boldness and purpose. I cannot possibly understand why you were so invested in me so early, but I will forever be indebted for it. To Jason and David: thank you for your generous mentorship and guidance throughout my time in the department, and especially as I navigated the NIH F99/K00 process. Your support opened doors I couldn't imagine (somewhat literally, given that I'm leaving to work with Mauricio, whom I would also like to acknowledge for being an absolute angel in a dark time). To my friends outside the lab - Camille, Ronan, and the many others I can't begin to name here - thank you for the laughter, encouragement, and grounding presence you've provided. And to my family: thank you for supporting me through the long hours and modest paychecks. Thank you for believing in the worth of what I've pursued.

"*Every new discovery is just a reminder - we're all small and stupid*"

TABLE OF CONTENTS

Page

ABSTRACT ii

DEDICATION iii

ACKNOWLEDGMENTS iv

LIST OF TABLES ix

LIST OF FIGURES x

CHAPTER

1. INTRODUCTION 1

    The Ubiquity and Relevance of Uncertainty in Social Cognition 1

    Limitations of Conventional Experimental Approaches 3

    Social and Non-Social Sources of Uncertainty 5

    The Role of Interpretive Perspectives in Uncertainty Resolution 6

    Appraisal and Neural Synchrony Within Diverging Perspectives 8

    The Moderating Role of Stimulus Complexity and Informativeness 13

    Contributions of the Present Work 15

2. METHODS 17

    Participants and Study Overview 17

        fMRI Appraisal Expression Study 17

        Sparsely Sampled Social Appraisal Study 19

        Social Appraisal Manipulation Study 20

    Experimental Design and Task Procedures 21

Stimulus Overview....21
Task Design - fMRI Appraisal Expression Study....21
Task Design - Sparsely Sampled Social Appraisal Study....24
Task Design - Social Appraisal Manipulation Study....25
Data Acquisition and Pre-Processing....26
Experimental Display and Appraisal Acquisition....26
Neuroimaging Acquisition....27
Appraisal Data Pre-Processing....28
Neuroimaging Pre-Processing....29
Anatomical Data Pre-Processing....30
Functional Data Pre-Processing....30
Anatomical Parcellation....34
Important Recurring Concepts and Computational Definitions....34
Appraisal Engagement....34
Appraisal Clustering....35
Appraisal Synchrony....37
Neural Synchrony....39
Stimulus Complexity....41
Informational Weight....43
Statistical Modeling and Analytic Strategy....44
Binary Logistic Regression....44
Linear Models....44
Hierarchical Linear Modeling....44

Intersubject Correlations 45
Correction for Multiple Comparisons 45
Open Access Statement 45
3. RESULTS 46
Appraisal Clustering Reflects Diverging Perspectives 46
Shared Perspective Enhance Appraisal Synchrony 47
Appraisal Complexity Amplifies Shared Perspective 48
Emotional Complexity Reduces Appraisal Synchrony 50
Appraisal Synchrony Reflects Cognitive Engagement, Not Inactivity 51
Informational Weight Synchronizes Appraisals Regardless of Perspective 52
Shared Perspectives Cannot Be Inferred from Neural Synchrony Alone 53
Social and Non-Social Appraisals Broadly Synchronize Brain Networks 54
Social Appraisals Drive Greater Neural Synchrony Than Non-Social 55
Neural Synchrony Predicts Social and Non-Social Appraisal Synchrony 57
Social Neural–Appraisal Synchrony Improves Within Perspective 59
Neural–Appraisal Synchrony Varies by Complexity Across Regions 60
Perspective and Complexity Co-Construct Appraisal-Neural Synchrony 61
4. DISCUSSION 64
Confirmation Bias and Heuristics 66
Shared Reality and Mentalizing 67
Interpreting Neural Findings in Naturalistic Contexts 68
Limitations 70
Future Directions 72

Conclusion 74

REFERENCES 75

APPENDIX...90

LIST OF TABLES

Table Page

1. Average Network Synchrony by ISC Analysis………………………………. 57
2. Appraisal-Neural Synchrony Parcels Moderated by Domain ………...…..…. 93
3. Social Appraisal-Neural Synchrony Parcels Moderated by Perspective …...... 94
4. Appraisal-Neural Synchrony Parcels Moderated by Complexity ……............ 95

LIST OF FIGURES

Figure Page

1. Reflective and Expressive Viewing 18
2. Task Design 22
3. Appraisal Engagement Trajectories 29
4. Appraisal Cluster Trajectories 47
5. The Effects of Complexities Upon Appraisal Synchrony By Perspective 49
6. The Effects of Complexities Upon Appraisal Synchrony................................51
7. Appraisal Engagement Predicts Synchrony 52
8. Informational Weight – Cluster Type Predicts Appraisal Synchrony 53
9. Domain-Specific Intersubject Correlation Values By Region.........................56
10. Domain-Specific Appraisal-Neural Synchrony Associations..........................58
11. Perspective-Sensitive Social Appraisal-Neural Synchrony 60
12. Complexity-Sensitive Appraisal-Neural Synchrony By Domain 63

CHAPTER 1

INTRODUCTION

The Ubiquity and Relevance of Uncertainty in Social Cognition

Whether encountering strangers for the first time or making decisions about long-trusted friends, social situations are often rife with uncertainty. This uncertainty can stem from incomplete information (Fiske, 1992), conflicting cues (Clark et al., 2018), or unpredictability in others' intentions, emotions, or future behavior (Fiske, 1992; Vives & FeldmanHall, 2018; Ybarra et al., 2010). Uncertainty may sometimes be easier to recognize and quantify from non-social sources - like actuarial risk assessments or betting odds - than from social sources (Ellsberg, 1961; Hertz et al., 2020; Kahneman & Tversky, 1978) because others may not disclose their emotions, goals, or beliefs (Frith & Frith, 2012). Even when cues are available, they may be inconsistent or subtly contradictory, creating conflict and uncertainty about the other's state of mind (Dovidio & Gaertner, 2000). Prejudice, for example, can involve a complex layering of conflicting cues (e.g., polite language paired with dismissive tone) that render others' intentions both ambiguous and cognitively demanding to interpret (Clark et al., 2018). Further complicating matters, others' behavior is often unpredictable (Kahneman & Tversky', 1978), especially in contexts featuring strategic decision-making or limited communication, where actors may conceal or withhold information to gain advantage (Neys et al., 2011). Individuals are left to reason under ambiguity rather than risk in such cases, as no clear probabilities can be assigned to possible outcomes (Deutsch, 1960; Hertz et al., 2020). These features (i.e., partial observability, mixed signals, and behavioral indeterminacy) make social uncertainty a persistent and cognitively demanding challenge in many situations.

Dealing with such uncertainty is an unavoidable reality of daily life, and its consequences are far-reaching. Social uncertainty in particular evokes aversive and distressing affective states (Birrell et al., 2011; Kagan, 1972), and psychologically-typical adults reliably demonstrate ambiguity avoidance in both economic (Ellsberg, 1961; R. Li et al., 2015; Trautmann et al., 2008) and interpersonal contexts. For example, individuals will incur personal costs to reduce uncertainty about how others will respond to their actions (Hertz et al., 2020). Uncertainty-elicited distress can rise to the level of clinical significance as well; particularly in individuals with anxiety, depression, and post-traumatic stress disorder (Carleton et al., 2012; Fetzner et al., 2013; Oglesby et al., 2016). Intolerance of uncertainty is a transdiagnostic feature of numerous psychiatric conditions, including anxiety, depression, PTSD, schizophrenia, and autism spectrum disorders, where uncertainty can become dysregulating and contribute to maladaptive appraisals and behaviors (Carleton et al., 2012; Fujino et al., 2016; Morriss et al., 2019). Even in non-clinical populations, lower tolerance of uncertainty predicts greater emotion regulation difficulties (Shu et al., 2021). Developmentally, adolescence marks a particularly sensitive period, during which heightened social uncertainty is linked to poor regulation, peer susceptibility, and risky decision-making (Chu et al., 2019; Sutter et al., 2013; Tymula et al., 2012). Adolescent responses to ambiguity diverge from those of adults (Blankenstein et al., 2016; R. Li et al., 2015), and chronic exposure to social uncertainty in youth predicts later vulnerability to anxiety and depression (Pagliaccio et al., 2022).

Given its profound impact on affect, decision-making, development, and psychopathology, understanding how people perceive, appraise, and resolve social uncertainty is a central challenge for psychology and neuroscience

Limitations of Conventional Experimental Approaches

Much of what is known about social uncertainty has been derived from economic paradigms such as the Trust Game or Ultimatum Game, in which participants engage with real or fictitious partners to make discrete, incentivized decisions (Alós-Ferrer et al., 2012; Alós-Ferrer & Farolfi, 2019). These tasks offer considerable experimental control and are useful for probing constructs like reciprocity, fairness, and belief updating (Brudner et al., 2021; Delgado et al., 2005; Fareri & Delgado, 2014). However, they are ultimately limited in their ability to model the ecologically valid, real-world contexts in which social uncertainty naturally arises. For instance, these tasks typically isolate individual trials, limit interaction to well-defined rules, and constrain participants' choices to simple economic outcomes- features not mirrored in the open-ended, dynamic, and multimodal nature of real-life social cognition (Friedman & Gustavson, 2022; Levy et al., 2021).

People often make social judgments through continuous appraisal of complex stimuli, often integrating information from multiple sensory modalities and over extended timescales. For example, interpreting whether someone is lying or whether a character is trustworthy unfolds gradually as the listener sifts through facial expressions, vocal intonation, background context, and evolving narrative details (Lauharatanahirun et al., 2021). These situations rarely come with known outcome probabilities or clearly defined options. Instead, they allow a broad set of possible interpretations and outcomes, which must be inferred and updated in real-time based on new evidence (Deutsch, 1960;

FeldmanHall & Shenhav, 2019). Trial-based paradigms, by contrast, lack temporally layered narratives, nuanced interpersonal dynamics, and evolving motivations, and they don't require resolving ambiguity over time as in everyday social interactions (Nastase et al., 2020). Despite this, many studies of social cognition continue to rely on highly structured tasks with minimalistic stimuli, measuring judgment outcomes in response to isolated and often decontextualized social cues (FeldmanHall & Shenhav, 2019; Lauharatanahirun et al., 2021). The strong causal inference and high replicability afforded by these approaches come at the expense of ecological validity. Naturalistic stimuli (e.g., narrative-based videos) offer a compelling alternative (Hari et al., 2015).

These stimuli enable researchers to approximate the dynamic, multimodal environments in which social cognition naturally unfolds, preserving temporal structure, social complexity, and contextual richness (Antony et al., 2021; Chen et al., 2017; Heusser et al., 2021; Mitchell et al., 2021; Song et al., 2021). Critically, video paradigms retain some of the experimental control characteristic of traditional designs, while incorporating more authentic complexity and temporal continuity (DuPre et al., 2020; Liberty S. Hamilton et al., 2020; Sonkusare et al., 2019). Video stimuli elicit strong subjective experiences (Westermann et al., 1996), evoke vivid sensory and emotional representations that mirror our own experiences (Goldberg et al., 2014; Saarimäki, 2021), and foster high engagement while yielding data that are readily comparable across individuals (Gross & Levenson, 1995; Hutcherson et al., 2005; Jääskeläinen et al., 2022). As such, they are well-suited for studying complex phenomena like social appraisal, empathy, and shared attention (Hasson et al., 2004; Hasson, Furman, et al., 2008; Hasson, Landesman, et al., 2008).

Thus, investigating the neural and behavioral dynamics of social uncertainty may require experimental designs that more closely mirror the environments in which uncertainty naturally arises.

Social and Non-Social Sources of Uncertainty

Uncertainty arises across a wide range of cognitive domains, including interpersonal inference (e.g., “Am I being told the truth?”) and perceptual ambiguity (e.g., “Was the traffic light red or yellow?”) (Blankenstein et al., 2016; Fairley et al., 2022; FeldmanHall & Shenhav, 2019). While both types of uncertainty are subject to appraisals, they differ in their sources and the cognitive strategies used to resolve them. Non-social uncertainty is often grounded in sensory ambiguity or probabilistic reasoning, and can frequently be modeled with well-characterized tasks such as perceptual discrimination, statistical inference, or reward maximization (Blankenstein et al., 2016; Ellsberg, 1961; F. Li et al., 2015). Some of the earliest applications of drift diffusion modeling, for example, relied upon appraisals of brightness and darkness within pixel patches (Ratcliff, 1978, 2002). In contrast, social uncertainty involves interpreting others’ hidden intentions, emotions, or future behavior, making it more difficult to quantify or externally verify, as previously noted (FeldmanHall & Shenhav, 2019). Despite the ubiquity of social uncertainty in everyday life, few studies have directly compared how people form certainty judgments across social vs. non-social domains, particularly using complex and naturalistic stimuli.

Emerging evidence suggests that social and non-social uncertainty rely on partially dissociable neural circuits, reflecting distinct underlying cognitive processes. Neuroimaging studies have shown that social certainty judgments recruit the inferior frontal gyrus (IFG), ventrolateral prefrontal cortex (vlPFC), precuneus, and anterior insula (AI) - regions often implicated in theory of mind, emotional salience, and social reasoning - whereas non-social ambiguity tends to engage the intraparietal sulcus (IPS), a region associated with perceptual integration and numerical estimation (Fairley et al., 2022; Martinez-Saito & Gorina, 2022). These differences may reflect the distinct demands imposed by the two domains: non-social tasks often emphasize quantifiable features and unimodal inputs, while social tasks demand inferential reasoning, reliance on prior schemas, and interpretation of ambiguous multimodal cues (Ma et al., 2022; Martinez-Saito & Gorina, 2022). However, these results primarily reflect findings from well-controlled, trial-based paradigms and may capture only a narrow set of regions involved in uncertainty appraisal, compared to the richer, more context-dependent appraisals made in daily life.

As a result, our understanding of how people generate, update, and regulate uncertainty in response to complex social and non-social information remains limited. Developing more ecologically valid frameworks to examine the cognitive and neural architecture of domain-specific and domain-general uncertainty is critical.

The Role of Interpretive Perspectives in Uncertainty Resolution

Uncertainty rarely exists in a vacuum; instead, individuals make sense of ambiguous information through the lens of interpretive hypotheses, shaped by prior beliefs, expectations, emotional state, and contextual framing. These interpretive perspectives guide attention, shape emotion regulation, and influence how individuals construct meaning over time, especially when faced with dynamic and complex social stimuli. Even when presented with identical inputs, observers often arrive at markedly different conclusions, a phenomenon underscored by the Rashomon effect and demonstrated empirically through variability in neural and behavioral responses during naturalistic tasks (Finn et al., 2018; Yeshurun et al., 2017).

Recent work has shown that interpretive divergence is not merely noise, but reflects systematic differences in schema activation and information valuation. For example, Yeshurun and colleagues (2017) found that giving participants different interpretive frames prior to a story significantly altered neural synchrony in higher-order areas, including the default mode network, suggesting that shared interpretive frameworks align cognitive processing across individuals. Similarly, Finn et al. (2018) demonstrated that individual differences in trait paranoia modulated synchrony and theory-of-mind-related activation during an ambiguous social narrative, highlighting the role of dispositional biases in shaping real-time social cognition. Relatedly, Bacha-Trams et al (2017) showed that even cultural background can influence functional network reconfiguration during narrative listening, further supporting the idea that internal frameworks, whether primed or intrinsic, fundamentally structure how we interpret ambiguous content.

To examine how interpretive perspectives influence uncertainty appraisals, I conducted a study in which participants were assigned roles designed to bias their interpretation (Mitchell et al., In Preparation). These roles were stimulus-relevant; either friend of the victim, friend of the accused, or detective. Participants provided continuous certainty ratings regarding a target character’s guilt while watching short, temporally segmented clips. These simple role assignments alone significantly shaped how subjects appraised information. For example, detectives and friends of victims were significantly more certain in their conclusions than friends of the accused. Friends of victims also reached firmer conclusions more rapidly than both detectives and friends of the accused. Furthermore, using a proxy for informational updating (i.e., area under the curve), I found that all of the roles responded similarly to clarifying information (i.e., information lacking ambiguity), but that ambiguous information was interpreted as uncertainty-resolving significantly more often among friends of the accused than friends of the victims. These results suggest that interpretive perspective not only biases initial expectations but also filters the perceived informativeness of subsequent evidence, leading to divergent uncertainty trajectories even in response to shared stimuli.

Appraisal And Neural Synchrony Within Diverging Perspectives

Complex social and cognitive experiences are inherently multidimensional, unfolding dynamically over time and shaped by an individual's unique expectations, goals, and prior knowledge. Such processes often elude traditional univariate neuroimaging approaches, which focus on mean activation levels and assume homogeneity across individuals. In contrast, pattern-based multivariate techniques such as Intersubject Correlation (ISC) provide a powerful framework for capturing how similar patterns of neural activity evolve across individuals exposed to shared stimuli (Hasson et al., 2004; Nastase et al., 2019). Because these analyses track correlated temporal patterns rather than mean signal intensity, they are especially sensitive to subtle or distributed neural dynamics, detecting consistent regional fluctuations that traditional univariate methods may overlook (Kriegeskorte et al., 2008; Popal et al., 2019).

ISC offers a window into *synchrony* - the degree to which two or more individuals exhibit similar patterns of neural, physiological, or behavioral activity over time in response to the same information. High intersubject neural synchrony is thought to reflect shared cognitive and emotional processing, with prior work linking synchrony to cooperation, empathy, agreement, and perspective-taking (Kinreich et al., 2017; Lahnakoski et al., 2014; Lu & Hao, 2019; Xu et al., 2020). Conversely, diminished synchrony has been observed in clinical populations, including individuals with autism spectrum disorder (Lyons et al., 2020) and anxiety disorders (X. Li et al., 2021), suggesting that synchrony can serve as a neurobiological marker of alignment or misalignment between individuals' internal representations of socially and emotionally meaningful content.

ISC is well-suited for analyzing narrative videos because it provides a model-free window into shared processing dynamics across individuals while respecting the temporal and contextual complexity of the stimulus (Antony et al., 2021; Hasson, Furman, et al., 2008). Rather than requiring explicit stimulus annotation or response modeling, ISC synchrony captures when individuals converge in their interpretations, attentional focus, or emotional responses during complex, naturalistic experiences. As such, synchrony serves as an index of normativity, consensus, and generalizability, especially when explicit task structure is minimal. By revealing when and where participants spontaneously align, synchrony highlights emergent properties of shared cognition and affect that are reliably evoked across observers, even in complex, naturalistic settings which may be difficult to specify a priori.

ISC is most often applied to passive viewing paradigms, during which subjects observing stimuli often without direction and without making explicit responses or judgments. Naturalistic viewing paradigms elicit complex, subjective appraisals that are often context-dependent and idiosyncratic (Ma et al., 2022), but these appraisals are rarely measured concurrently with neural activity. Most studies examine how neural synchrony correlates with *downstream outcomes,* such as later decision-making or memory recall, rather than directly indexing the *appraisal process itself* (Levy et al., 2021). This represents a missed opportunity, particularly when studying phenomena like uncertainty, where moment-to-moment assessments may fluctuate widely across individuals. Without accurately extracting and reliably modeling both stimuli features (Simony & Chang, 2020) and the subjective experiences of participants (Saarimäki, 2021), researchers must assume or infer the presence (or absence) of these higher-order cognitive assessments or reactions. Manual and automated annotation approaches solve some of the issues for documenting tangible stimuli features (de la Vega et al., 2022). However, standardizing the capture of subjective experiences is uniquely challenging and comparatively less developed (Jääskeläinen et al., 2022).

Recent work has advocated for the integration of continuous behavioral sampling with ISC analyses in dynamic, socially meaningful tasks (Levy et al., 2021; Mauss et al., 2011; Mitchell et al., 2025). Continuous self-report rating approaches have been used extensively beyond neuroimaging as a high-resolution representation of subjective experiences (Fredrickson & Kahneman, 1993; Jeremy Peterman & Peterman, 1940; Levenson & Gottman, 1983; but see Ruef & Levenson, 2007 for a review). These approaches transform a passive viewing experience (i.e., observing with no direction or while collecting any explicit appraisal metric) into an active process (i.e., observing while completing a continuous appraisal task) by giving subjects an explicit question to consider or instructions to follow while watching the stimulus. These guidelines likely narrow focus and circumscribe cognition (Hutcherson et al., 2005) relative to passive viewing paradigms, allowing researchers to gain a window into a specific subjective assessment at the cost of allowing subjects to entertain a wider berth of subjective questions. Consequently, active viewing paradigms may yield greater experimental control at the cost of less ecological validity than passive viewing paradigms. However, researchers have expressed concern that the act of rating itself may fundamentally alter the cognition, and thus neural activity, occurring while subjects view a stimulus (Jääskeläinen et al., 2022; Nummenmaa et al., 2012; Saarimäki, 2021), akin to that demonstrated in the affective labeling literature. Support for this concern is mixed, though, as the literature often cited either did not use continuous ratings and dynamic stimuli (Lieberman et al., 2007; Taylor et al., 2003) or contrasted significantly different viewing conditions (Borja Jimenez et al., 2020; Hutcherson et al., 2005) confounding the act of rating with differences in instruction (i.e., differences may stem from being given a focus rather than rating itself). The affective labeling literature itself may provide evidence contrary to this interpretation, as non-affective labeling via gendering (Lieberman et al., 2007) or other descriptors (Lieberman et al., 2011) often fails to demonstrate similar consequences as affective labeling upon one's self-reported evaluations (Torre & Lieberman, 2018). Other studies found minimal disruption to experiential and physiological measures while expressively engaged (Hutcherson et al., 2005; Mauss et al., 2005; Wagner et al., 2020). Furthermore, my examination contrasting active and passive viewing without confounding rating and instruction differences found subtle differences in activation and synchrony in some low-level sensory and attention regions, but failed to demonstrate consistent substantive differences in higher-order cognitive networks (Mitchell et al., 2025).

There are several advantages or strengths that expressive engagement - capturing continuous self-report ratings during first exposure to a stimulus – might offer, particularly when studying long, complex, or socially dynamic experiences. Retrospective evaluations often suffer from fatigue, memory distortion, and hindsight bias, especially when participants must recall subtle, ambiguous, or fleeting aspects of an experience (Jääskeläinen et al., 2022; Stasiak et al., 2023). These limitations are amplified when stimuli unfold over extended periods or involve information-rich social interactions, where real-time judgments may be shaped by idiosyncratic attentional patterns and expectations (Fayn et al., 2021; Jääskeläinen et al., 2022). Andric and colleagues (2016) observed differences in network configurations of neural activity between repeated showings of the same stimulus, suggesting that higher-level neural processing differs considerably even when explicit ratings of subjective experiences look similar. Passive and reflective (i.e., watching a stimulus once without rating and rewatching again later while continuously rating) techniques often fail to preserve the nuanced, evolving nature of appraisals that occur in response to uncertainty or ambiguity. For example, surprise or fear may be difficult to replicate during post-hoc ratings due to information asymmetry between initial and repeated exposures (Stasiak et al., 2023). Expressive engagement, by contrast, retains the fidelity of initial responses and avoids confounds introduced by memory decay or interpretive reconstruction. Furthermore, for stimuli that naturally prompt hypothesis generation - such as ambiguous narratives or mystery-based content - the cognitive demands of passive viewing may already resemble those of active engagement. That is, participants may spontaneously attend to the same features or questions that expressive paradigms explicitly ask them to rate. Thus, expressive engagement not only provides a richer and more accurate account of subjective appraisal dynamics, but also enhances the interpretability of neural data by aligning it with the time course of evolving judgments.

Neural synchrony during social narrative comprehension may thus reflect not just shared sensory input, but shared *appraisal trajectories*; the ways in which individuals converge (or diverge) in how they understand, evaluate, and respond to complex, uncertain situations. By coupling time-resolved self-reports (e.g., moment-by-moment certainty ratings) with naturalistic fMRI data, researchers can identify not just *where* participants' brains synchronize, but *when* that synchrony aligns with shared subjective appraisals. This approach enables a novel extension of ISC: rather than treating synchrony as an outcome, it becomes a predictor of interpretive convergence, allowing for direct mapping between brain activity and shared psychological states over time.

The Moderating Role of Stimulus Complexity and Informativeness

Complex social and cognitive experiences unfold over time in response to dynamic, multidimensional inputs. Rather than operating uniformly across a stimulus, appraisal processes are likely to fluctuate in relation to the evolving structure and meaning of the input. Two key properties of naturalistic stimuli, complexity and informativeness, provide powerful proxies for quantifying this variability in cognitive demands. Entropy, broadly defined as the unpredictability or uncertainty within an event (Shannon, 1948), reflects the complexity or ambiguity of available information, while informativeness captures the diagnosticity of an event for resolving a particular hypothesis or interpretive frame (Deutsch, 1960; FeldmanHall & Shenhav, 2019). Recent research suggests that these dimensions dynamically shape perception, attention, and memory, and may play a critical moderating role in structuring when and how interpretive synchrony emerges across individuals.

In both perceptual and cognitive domains, entropy has been shown to influence subjective experience and neural engagement. For instance, visual arrays with low color entropy are perceived as more numerous than high-entropy arrays, suggesting that more structured, coherent inputs can bias magnitude estimation (Qu et al., 2022). In the auditory domain, individuals can detect and discriminate entropy in tone sequences, with consistent perceptual thresholds emerging across listeners (Zhu, 2023). In a neuroimaging context, entropy has been shown to modulate hippocampal engagement: sequences with high temporal unpredictability (i.e., high entropy) elicit stronger anterior hippocampal activation, reflecting the brain's sensitivity to contextual uncertainty during learning (Strange et al., 2005). These findings demonstrate that entropy is not only behaviorally relevant but also recruits memory and predictive processing systems when information is less structured and more ambiguous.

Interpretation may be informed by heuristics or schemas rather than deliberative analysis under these complex conditions. For instance, when details of a crime are unclear, individuals tend to incorporate schema-consistent errors into their recollections that align with their existing expectations (Tuckey & Brewer, 2003). Similarly, when sentences are structurally ambiguous, readers use narrative-based heuristics (e.g., noun–verb–noun scripts) to infer missing information and resolve meaning (Dwivedi et al., 2018). These findings align with dual-process models which argue that when stimuli are unclear or cognitive resources are limited, individuals default to fast, heuristic shortcuts informed by prior knowledge or expectation (Chaiken & Ledgerwood, 2012). When evidence is insufficient, people may allow schemas or heuristics to fill informational voids, thus increasing synchronization among those already sharing the same perspective.

At the same time, informativeness (i.e., the degree to which an event clarifies an evolving hypothesis) has been shown to amplify attention, memory encoding, and behavioral alignment, as well. In naturalistic paradigms, individuals tend to synchronize more strongly in their neural responses (Nastase et al., 2019; Yeshurun et al., 2017) and social judgments (Mitchell et al., In Preparation) when stimuli contain diagnostic social information, such as morally charged or emotionally pivotal moments. Supporting this, event boundaries, plot twists, and character revelations in narrative contexts consistently evoke greater intersubject correlation and memory consolidation (Baldassano et al., 2017; Chen et al., 2017; Heusser et al., 2021).

These findings suggest that appraisal synchrony is not temporally uniform but rather emerges most robustly at moments of high entropy (where multiple interpretations compete) and high informativeness (where interpretations can be resolved). Entropy and informativeness thus jointly shape how individuals parse complex stimuli, determining the degree to which their attention, memory, and evaluative processes converge. By explicitly modeling these stimulus properties, researchers can better understand the temporal dynamics of shared interpretation, as well as the cognitive architecture that supports flexible and coordinated meaning-making under uncertainty.

Contributions of the Present Work

In this dissertation, I propose a novel approach for studying how people form, update, and converge upon social and non-social judgments under uncertainty in ecologically valid contexts. Across three studies, I integrate continuous self-report, interpretive framing manipulations, intersubject correlations, and time-resolved modeling of stimulus complexity to capture the evolving nature of social and non-social appraisal in response to naturalistic video narratives. This work introduces methodological advances, including a sliding window approach to quantifying appraisal synchrony, manipulations to shape interpretive hypotheses, and the application of hierarchical linear modeling to assess the associations between concurrent intermodal synchronies (i.e., neural and appraisal synchrony) over time. Furthermore, I investigate how the brain-behavior relationship between neural synchrony and appraisals is moderated by both internal and external contextual factors. Critically, I demonstrate that social appraisals reliably cluster into unique perspectives, that subjects synchronize appraisals over time within perspective, that informational complexities and weights have differing effects upon intersubject appraisal synchrony, that social and non-social appraisals synchronize broad neural networks and recruit both domain-specific and domain-general circuitry that is sensitive to stimulus complexity. These findings suggest that synchrony is not a static marker of shared experience but a dynamic index of interpretive coherence that is modulated by both top-down framing and bottom-up stimulus complexity. Together, this research pushes the field beyond traditional trial-based or post-hoc paradigms and provides a richer, temporally-sensitive account of how individuals make sense of ambiguous, socially-relevant situations as they unfold.

CHAPTER 2

METHODS

Participants and Study Overview

Across three studies, I recruited a total of 178 participants to examine how individuals form, update, and align social and non-social appraisals during naturalistic decision-making. All participants were fluent English speakers with normal or corrected-to-normal vision and hearing, free of self-reported psychological, neurological, or developmental disorders, and provided informed consent in accordance with protocols approved by the relevant Institutional Review Board.

fMRI Appraisal Expression Study. Thirty-five participants (20 female, 15 male; age range: 18–44 years, $M = 24.5$, $SD = 5.5$; median age: 22 years) completed an fMRI study at Temple University between May 2022 and June 2023. Participants were recruited from the greater Philadelphia area. Five individuals were excluded for excessive head motion (1), prior familiarity with the stimulus (1), non-compliance (1), or incomplete data due to technical issues (2). The final sample included 4 left-handed individuals; handedness was not used as an exclusion criterion but was documented and included as a covariate where appropriate. Approximately 54.3% of the sample identified as non-Hispanic White, 5.7% as Hispanic White, 31.4% as Asian, and 8.6% as Black. MRI experience varied, with 11 participants reporting no prior scans and 5 reporting five or more prior scans. Participants were compensated $25 per hour for a two-hour visit.

Participants viewed a 45-minute episode of a naturalistic murder mystery drama while undergoing functional neuroimaging. Each participant continuously rated how much each moment of the episode contributed to their appraisal of the guilt of a primary character ("expressive viewing") for one half of the episode and passively considered the same question without rating ("reflective viewing") for the other half (Mitchell et al., 2025) (**Figure 1**). Assignment of which half received expressive versus reflective engagement was pseudorandomized across participants. In a separate run, participants also completed an analogous non-social task in which they continuously rated their certainty about relative luminance changes while watching a different episode from the same series.

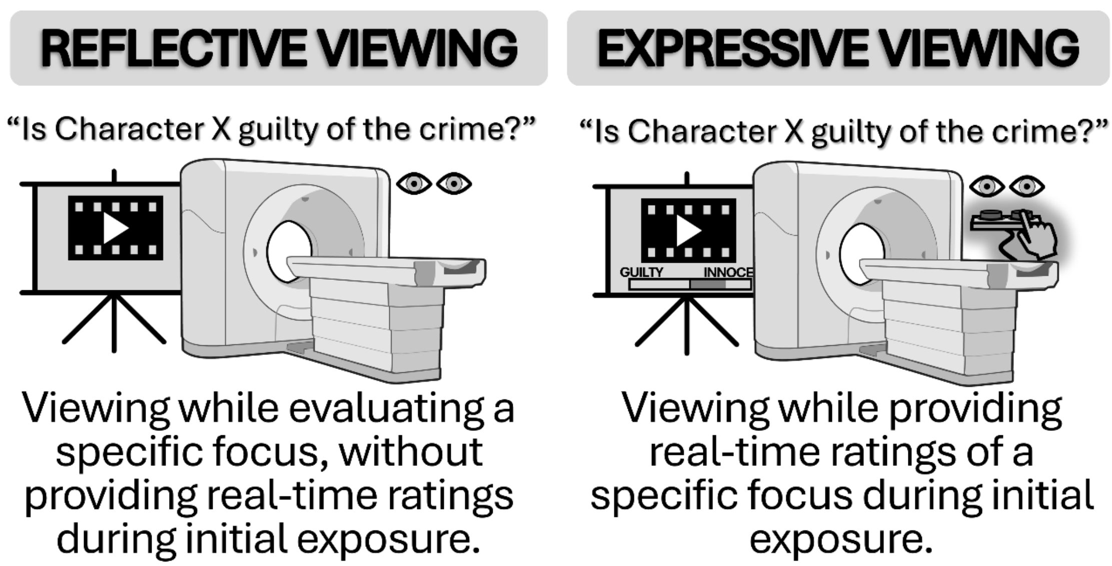

Figure 1. Reflective and Expressive Viewing Participants engaged in two distinct modes of viewing while undergoing fMRI. In the Reflective condition, participants passively considered the focal question (e.g., appraising a character's guilt) without providing any explicit response. In the Expressive condition, participants continuously reported their appraisals (e.g., via a rating scale), requiring them to externalize their moment-to-moment interpretations.

These time-varying continuous ratings reflect appraisal trajectories (i.e., subjective, evolving evaluations of stimulus content, whether moral (e.g., a character's guilt) or perceptual (e.g., brightness)). Although the term "appraisal" is often situated within affective science, here I adopt its broader cognitive meaning: the dynamic evaluation of unfolding information under conditions of uncertainty. Appraisal, as classically defined (Folkman & Lazarus, 1986; Smith & Ellsworth, 1985), describes the process by which individuals assess the significance of a stimulus relative to their goals and well-being. In our paradigm, continuous ratings, whether assessing moral judgments such as guilt and innocence or perceptual qualities like luminance contrast, reflect appraisals that are subjective (person-specific), dynamic (changing over time), interpretive (shaped by internal models of the situation), and cognitively mediated (not simple reflexive responses). These characteristics map directly onto appraisal as a psychological process.

This design enabled us to disentangle neural dynamics related to active appraisal expression, while also probing for generalizable mechanisms of information processing across social and non-social domains.

Sparsely Sampled Social Appraisal Study. Ninety participants (45 female, 45 male; age range: 18–65 years, $M = 37.6$, $SD = 12.8$; median age: 36 years) completed a web-based behavioral study between January and May 2025. Participants were recruited via Prolific and screened for high prior task approval rates (≥95%), current residence in the US or UK, and no hearing or language difficulties. Of the 105 individuals initially recruited, 15 were excluded for failing attention checks (3), reporting prior familiarity with the stimulus (4), or non-compliance, defined as low response variability across timepoints based on the standardized first derivative of their rating timecourse (8). The final sample was 73.3% non-Hispanic White, 6.7% Hispanic White, 6.7% Asian, and 11.1% Black. Participants completed the study in approximately 75 minutes and were compensated $10 per hour.

This study employed a sparse sampling approach - a design in which data are collected intermittently rather than continuously (Hasson et al., 2012; Sonkusare et al., 2019) - to measure appraisals about multiple characters at selected moments throughout a naturalistic video. The design prioritized breadth over temporal resolution, aiming to assess how viewers maintained and revised complex hypotheses under ambiguity. Complex appraisals may be interdependent (e.g., suspicion toward Jonathan's wife, Grace, may decrease belief in Jonathan's guilt), or uncorrelated (e.g., viewers may "hedge their bets", maintaining and updating competing hypotheses over time rather than committing to a single interpretation). These strategies may reflect implicit social comparisons and context-dependent bias in evaluative processing (Fiske et al., 2007; Nisbett & Wilson, 1977) or be in line with resource-rational or Bayesian models of social inference (Gershman et al., 2015; Jern et al., 2014), respectively. This design allowed us to model simultaneously-held, multidimensional appraisals. By tracking a broader berth of information at fewer timepoints, rather than a single focus with high resolution, I can better assess how decision-makers respond to the complexity and ambiguity signals inherent in the naturalistic stimuli.

Social Appraisal Manipulation Study. Twenty-three participants (12 female, 11 male; age range: 23–60 years, *M* = 37.9, *SD* = 10.8; median age: 33 years) completed a separate online study in May 2025 designed to evaluate how top-down framing shapes moment-to-moment appraisal. Thirty-three participants were recruited via Prolific, with 10 excluded due to technical issues (3) or non-compliance as defined by the same response variability criterion used in the sparse sampling study (7). The final sample was 60.7% non-Hispanic White, 13.0% Hispanic White, 13.0% Asian, and 8.7% Black.

In this study, participants were explicitly told that a specific character was the perpetrator before viewing the stimulus - effectively providing a “spoiler” - and then asked to continuously rate the strength of the evidence supporting that character’s guilt. This design allowed us to examine how individuals integrate new information through the lens of a strong prior belief and offered a high-resolution, dynamic measure of appraisal congruence with the stimulus.

Experimental Design and Task Procedures

Stimulus Overview. All studies employed the same core stimulus: a 44 minute 34 second episode of the HBO murder mystery series *The Undoing* (Episode 4, original airdate: 11/15/2020). This episode was selected for its strong narrative arc, multidimensional character development, and progressive revelation of morally and legally relevant information - features well-suited for studying evolving appraisal processes under conditions of uncertainty. The episode was edited to remove two scenes featuring sensitive or potentially offensive dialogue and to obscure a brief moment of gore; these changes preserved narrative continuity while minimizing potential distress or distraction. Stimulus delivery varied across studies depending on condition-specific manipulations but was preceded in all cases by a briefing that included narrative context and character background. For social judgment tasks, characters’ names, photos, and prior context were presented in a counterbalanced order to avoid lateral or sequential bias.

Task Design - fMRI Appraisal Expression Study. Participants first completed a brief training exercise to ensure fluency with the MR-compatible response device, which was operated using the right hand. This practice task mirrored the structure of the main experiment and served to stabilize performance; a necessary step given that continuous self-report tasks often exhibit a learning curve in early trials (Kimberley et al., 2008).

The primary task divided the stimulus into two equal halves (22 minutes, 17 seconds each) and presented it sequentially across two functional runs (**Figure 2A**). Prior to viewing, participants were pseudo-randomly assigned to one of two conditions using dynamic allocation, which weighted assignment probabilities to balance prior enrollments. Each participant continuously rated their certainty in a character's guilt or innocence for one half of the episode (expressive condition), and watched the other half without providing input but while considering the same evaluative judgment (reflective condition) (**Figure 2B**).

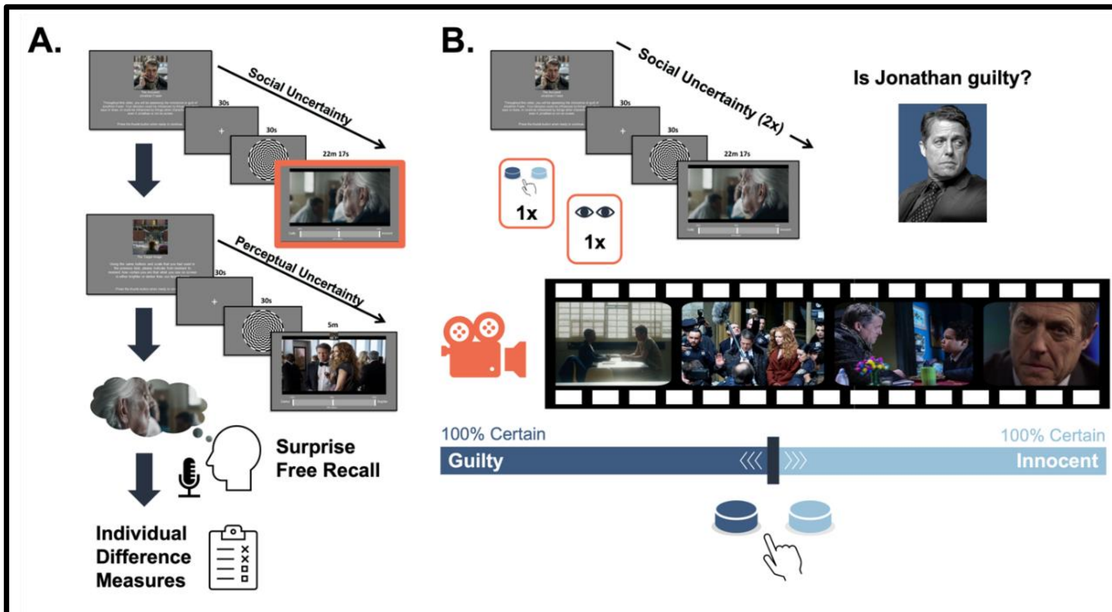

Figure 2. Task Design <u>A)</u> Subjects completing the fMRI Appraisal Expression Study completed 4 functional runs and a several individual difference measures. <u>B)</u> During the social runs, subjects watched one half of the stimulus expressively and the other reflectively, consistently considering and/or rating their appraisals regarding whether the target character, Jonathan, was guilty of the accused crime.

During the expressive condition, participants used a two-button interface to adjust a horizontal, bipolar scale displayed beneath the video. The scale ranged from 100% certain of guilt (left pole) to 100% certain of innocence (right pole), with the default starting position set to 0% (undecided). Pressing the index-finger button shifted the scale leftward by 5%, while the middle-finger button moved it rightward by the same increment. Of the final sample, 20 participants rated the first half of the episode, and 15 rated the second.

Following the social appraisal task, 30 participants completed an additional functional run targeting non-social certainty judgments. Five subjects had completed a different non-social task and are excluded from these analyses (See **Appendix**). Specifically, they continuously rated the perceived luminance of each video frame in a 5-minute excerpt from a different episode of *The Undoing* (Episode 1, original airdate: 10/25/2020). This episode was selected to preserve continuity in cinematography, character appearances, and general narrative tone while avoiding plot overlap. Audio was removed to prevent any lingering narrative effects and replaced with neutral, copyright-free piano music. A single reference image, positioned above the video for the duration of the task, served as an anchor for brightness comparisons. This image was selected as the frame closest to the median luminance value within the clip, such that approximately half of the remaining frames were brighter and half darker. Framewise luminance values were calculated using a standard formula (Poynton, 2003) implemented in R. This task was designed to parallel the temporal dynamics of the social judgment task while isolating domain-general processes supporting perceptual certainty estimation.

At the conclusion of all viewing tasks, participants underwent a surprise free recall task while still in the scanner, followed by task-related and individual difference measures outside the scanner. These latter assessments were not directly relevant to the current analyses and are not discussed further in this dissertation.

Task Design - Sparsely Sampled Social Appraisal Study. Participants first provided informed consent, completed a comprehension check, and reviewed character and narrative background materials identical to those used in the neuroimaging study. To mitigate potential lateral biases, the order and screen-side presentation of character portraits and accompanying text were counterbalanced across participants.

The primary task consisted of a continuous video viewing experience interrupted at pre-scheduled breakpoints. At each break, the video paused and participants were prompted to rate one of seven key characters using a slider scale ranging from "100% certain guilty" to "100% certain innocent." Each character appeared multiple times throughout the session, and a visual progress bar guided participants through the rating sequence. The order of characters was randomly determined for each subject but held constant across their session.

Participants were instructed to update their judgments based on any relevant cues from the video (e.g., dialogue, behavior, or off-screen events) that shifted their interpretation, even subtly. To encourage temporally contingent updates rather than isolated judgments, each character's rating interface was anchored to the value the participant had most recently assigned to that character (e.g., a previously submitted "60% guilty" rating for Jonathan would appear as the default position on the slider during the next rating).

After the main task, participants completed a battery of validated individual difference measures, including the Need for Closure Scale (NFCS), Intolerance of Uncertainty Scale (IUS), and State-Trait Anxiety Inventory (STAI), along with demographic and task-specific questions. These follow-up assessments were collected for broader research purposes and are not discussed further in this dissertation.

Task Design - Social Appraisal Manipulation Study. Participants first practiced using the continuous rating interface by completing a brief, custom instructional video tailored to the task structure. After reviewing the same background information presented in the previous studies, each participant was explicitly told that one of four characters (i.e., Jonathan Fraser, Grace Fraser, Franklin Reinhardt, or Fernando Alves) was responsible for the central crime. These characters were selected based on being the most frequently suspected across prior studies.

Participants then completed the primary task, in which they continuously rated how informative each moment of the video was with respect to the hypothesis that the designated character (i.e., the one they had been told was guilty) had committed the crime. Informative moments were defined as those offering new or compelling evidence supporting or contradicting that character's guilt, while uninformative moments were unrelated to the hypothesis. Participants were encouraged to base their ratings on their own evolving impressions and reminded that there were no right or wrong answers.

Ratings were provided using keyboard inputs and updated whenever participants' perceptions of informativeness changed, even subtly. The scale ranged from 0% (completely uninformative) to 100% (extremely informative), and was continuously visible beneath the video. Ratings were sampled continuously and recorded independently of user interaction, ensuring a complete and uninterrupted time series aligned with the stimulus timeline.

Data Acquisition and Pre-Processing

Experimental Display and Appraisal Acquisition. While many tools exist for collecting continuous self-report ratings (e.g., Girard & Wright, 2018), few offer the combination of low computational overhead, broad device compatibility, and seamless deployment needed for dynamic video-based studies across diverse testing environments. As such, my studies employed custom-built experimental paradigms optimized for continuous self-report acquisition during dynamic video presentation. Two software frameworks were used depending on study context: the neuroimaging study was implemented in Python (v3.8.13) (van Rossum, 1995) using PsychoPy (v2021.2.3) (Peirce et al., 2019), while both online studies (the sparse hypothesis sampling and hypothesis manipulation studies) were developed in JavaScript using jsPsych (v7.0) (De Leeuw et al., 2023) with Pavlovia integration, enabling seamless remote deployment and browser-based control.

In the neuroimaging study, participants provided ratings using an MR-safe five-button response box (Psychology Software Tools) held in the right hand. During pilot testing, this button box proved more stable and reliable than an alternative joystick interface, which was prone to overshooting or accidental input. Rating adjustments registered only upon button release to better isolate intentional changes and limit noise related to motor activity. Rating data were sampled at the native frame rate of the video (24 Hz). Special attention was paid towards audio delivery to ensure subjects could hear in the noisy fMRI environment (See **Appendix**).

For the online studies, participation required a desktop or laptop with a supported browser (e.g., Chrome, Firefox, Safari), audio playback capabilities, and either a keyboard or mouse for input. To ensure data quality, participants completed a series of device and environment checks before beginning the task, including full-screen enforcement and audiovisual readiness assessments. Stimuli were segmented into ~67-second chunks and preloaded in advance of playback to prevent memory overload or network buffering issues. Button presses were buffered to reduce accidental double-clicks, and all responses were timestamped using a custom logging function. Final data were automatically uploaded to Pavlovia's servers for secure storage.

In the sparse sampling study, participants rated character guilt at 34 pre-determined breakpoints distributed across the video. These points were assigned using an algorithmically constrained random sampling procedure designed to achieve uniform coverage while minimizing disruption. Full details of the break assignment procedure are provided in **Appendix**.

In the manipulation study, participants continuously rated the informativeness of the stimulus relative to a given guilt hypothesis. As jsPsych does not natively support high-frequency continuous rating input, I developed a custom plugin (Mitchell, 2024/2024) that recorded real-time slider movements at up to 24 Hz. Ratings were controlled using keyboard keys ('2' to decrease, '3' to increase) or via mouse input.

Neuroimaging Acquisition. fMRI scanning was performed at Temple University using a 3T Siemens Tim Trio MRI system and a 20-channel head coil. Each subject completed one high-resolution T1-weighted structural image and four functional runs. One of these runs (i.e., free recall) is beyond the purview of this manuscript. The acquisition parameters for the relevant T2* EPI BOLD sequences were acquired at a 3 mm slice thickness, a TR = 2000 ms; TE = 25 ms; flip angle of 75 degrees, and a FOV = 1680 x

1680 mm. A 30s audiovisual stimulus buffer (a rotating checkered pattern paired with pink noise generated using Audacity) preceded the stimulus of each run. Without a stimulus buffer, the global arousal response that video stimuli often elicit may have occurred during our stimulus and would have resulted in having to truncate neural data (Chen et al., 2017). Including fixation, stimulus buffer, and stimulus, between 729 and 759 3D volumes of the whole brain were collected (variance was due to adjustments regarding the length of fixation). Between each functional run, an accelerated T1-weighted image was collected to adjust functional alignment of the field of view as needed.

Appraisal Data Pre-Processing. All continuous appraisal time courses were preprocessed to ensure consistency across studies and to enhance interpretability of temporal dynamics. For comparability with the neuroimaging data in Study 1, all ratings were first downsampled to 0.5 Hz, matching the repetition time (TR = 2s) of the fMRI acquisition. This yielded 669 evenly spaced timepoints across the full 44-minute, 34-second stimulus for each participant. To account for individual differences in scale use and to emphasize within-subject fluctuations over time, all rating trajectories were z-standardized at the individual level. This transformation normalized the data while preserving the temporal structure of appraisals. To improve data quality in the behavioral studies (Studies 2 and 3), I implemented an additional quality control procedure based on the standardized first derivative of the appraisal time course. I refer to this as *Appraisal Engagement*. Participants with low overall variability (variance < 0.1) were presumed to have disengaged from the task (e.g., producing flat or unchanging responses), while those with excessive variability (variance > 5) were flagged as potential outliers due to erratic or noise-prone responding. Visual inspection of these cases confirmed the reliability of these thresholds in identifying noncompliant trajectories. After applying these criteria, 8 participants were excluded from Study 2, and 2 from Study 3, yielding final samples of 90 and 23, respectively, consistent with my pre-registered attrition tolerance. Examples of each are visible in **Figure 3**.

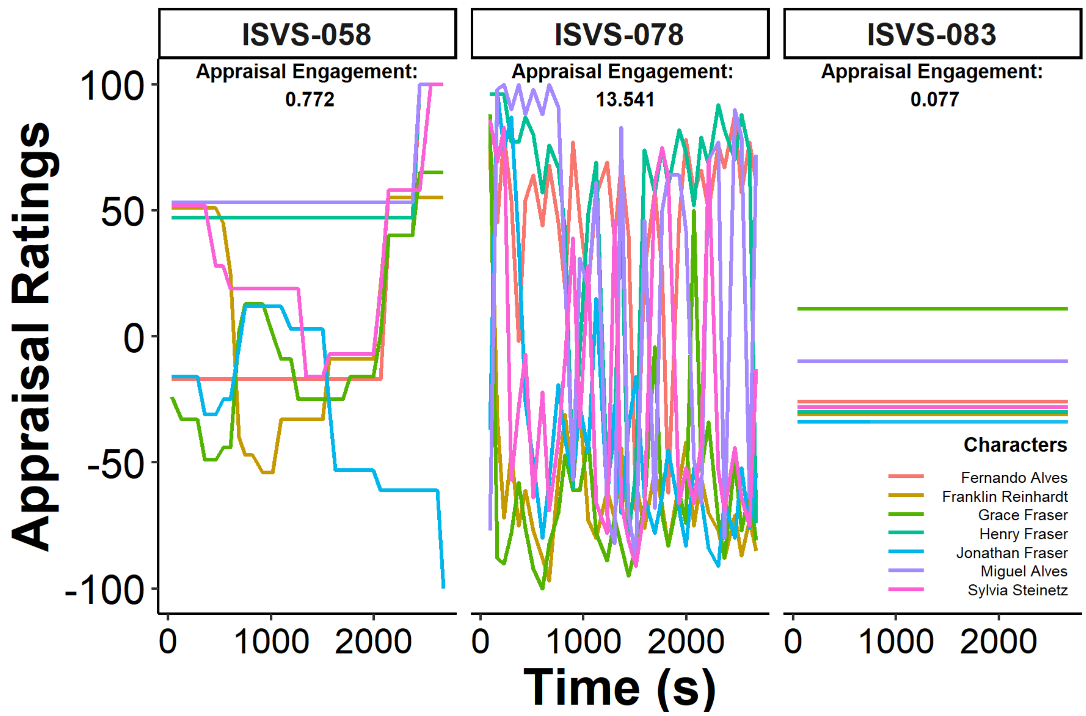

Figure 3. Appraisal Engagement Trajectories Appraisal rating over time from three subjects who participated in the Sparsely Sampled Social Appraisal Study are visualized. Subject ISVS-058 represents the median appraisal engagement value. ISVS-078 represents the subject closest to the upper boundary of our appraisal engagement cutoff (i.e., > 5.0. ISVS-083 represents the subject closest to the lower boundary of our appraisal engagement cutoff (i.e., < 0.1). As such, subjects with values greater than those cutoffs were excluded from further analyses.

Neuroimaging Pre-Processing. I first converted all MRI data from DICOM to BIDS-formatted NIfTI files using heudiconv [v0.11.3] (Halchenko et al., 2021). Neuroimaging data was pre-processed with the standard fMRIPrep [v20.2.6] (Esteban et al., 2017, 2019) pipeline within a Docker [v19.03.12] container to maintain generalizability, which is based on Nipype 1.7.0 (Gorgolewski et al., 2011).

Anatomical Data Pre-Processing. The T1-weighted (T1w) image was corrected for intensity non-uniformity (INU) with N4BiasFieldCorrection (Tustison et al., 2010), distributed with ANTs 2.3.3 (Avants et al., 2008), and used as T1w-reference throughout the workflow. The T1w-reference was then skull-stripped with a Nipype implementation of the antsBrainExtraction.sh workflow (from ANTs), using OASIS30ANTs as target template. Brain tissue segmentation of cerebrospinal fluid (CSF), white-matter (WM) and gray-matter (GM) was performed on the brain-extracted T1w using fast (FSL 5.0.9, Zhang et al., 2001). Volume-based spatial normalization to one standard space (MNI152NLin2009cAsym) was performed through nonlinear registration with antsRegistration (ANTs 2.3.3), using brain-extracted versions of both T1w reference and the T1w template. Spatial normalization was performed using the ICBM 152 Nonlinear Asymmetrical template version 2009c [Fonov et al., 2009; TemplateFlow ID: MNI152NLin2009cAsym].

Functional Data Pre-Processing. For each of the 3 BOLD runs per subject, a reference volume and its skull-stripped version were generated using a custom fMRIPrep methodology. Susceptibility distortion correction (SDC) was omitted. The BOLD reference was then co-registered to the T1w reference using flirt (FSL 5.0.9, Jenkinson & Smith, 2001) with the boundary-based registration (Greve & Fischl, 2009) cost-function. Co-registration was configured with nine degrees of freedom to account for distortions remaining in the BOLD reference. Head-motion parameters with respect to the BOLD reference (transformation matrices, and six corresponding rotation and translation parameters) are estimated before any spatiotemporal filtering using mcflirt (FSL 5.0.9, Jenkinson et al., 2002). BOLD runs were slice-time corrected to 0.965s (0.5 of slice acquisition range 0s-1.93s) using 3dTshift from AFNI 20160207 (Cox & Hyde, 1997). The BOLD time-series (including slice-timing correction when applied) were resampled onto their original, native space by applying the transforms to correct for head-motion. These resampled BOLD time-series will be referred to as preprocessed BOLD in original space, or just preprocessed BOLD. The BOLD time-series were resampled into standard space, generating a preprocessed BOLD run in MNI152NLin2009cAsym space.

Several confounding time-series were calculated based on the preprocessed BOLD: framewise displacement (FD), DVARS and three region-wise global signals. FD was computed using two formulations following Power (absolute sum of relative motions, Power et al., 2014) and Jenkinson (relative root mean square displacement between affines, Jenkinson et al., 2002). FD and DVARS are calculated for each functional run, both using their implementations in Nipype (following the definitions by Power et al. 2014). The three global signals are extracted within the CSF, the WM, and the whole-brain masks. Additionally, a set of physiological regressors were extracted to allow for component-based noise correction (CompCor, Behzadi et al., 2007). Principal components are estimated after high-pass filtering the preprocessed BOLD time-series (using a discrete cosine filter with 128s cut-off) for the two CompCor variants: temporal (tCompCor) and anatomical (aCompCor). tCompCor components are then calculated from the top 2% variable voxels within the brain mask. For aCompCor, three probabilistic masks (CSF, WM and combined CSF+WM) are generated in anatomical space. The implementation differs from that of Behzadi et al. in that instead of eroding the masks by 2 pixels on BOLD space, the aCompCor masks are subtracted a mask of pixels that likely contain a volume fraction of GM. This mask is obtained by thresholding the corresponding partial volume map at 0.05, and it ensures components are not extracted from voxels containing a minimal fraction of GM. Finally, these masks are resampled into BOLD space and binarized by thresholding at 0.99 (as in the original implementation). Components are also calculated separately within the WM and CSF masks. For each CompCor decomposition, the k components with the largest singular values are retained, such that the retained components' time series are sufficient to explain 50 percent of variance across the nuisance mask (CSF, WM, combined, or temporal). The remaining components are dropped from consideration. The head-motion estimates calculated in the correction step were also placed within the corresponding confounds file. The confound time series derived from head motion estimates and global signals were expanded with the inclusion of temporal derivatives and quadratic terms for each (Satterthwaite et al., 2013). Frames that exceeded a threshold of 0.5 mm FD or 1.5 standardised DVARS were annotated as motion outliers. All resamplings can be performed with a single interpolation step by composing all the pertinent transformations (i.e. head-motion transform matrices, susceptibility distortion correction when available, and co-registrations to anatomical and output spaces). Gridded (volumetric) resamplings were performed using antsApplyTransforms (ANTs), configured with Lanczos interpolation to minimize the smoothing effects of other kernels (Lanczos, 1964). Non-gridded (surface) resamplings were performed using mri_vol2surf (FreeSurfer).

Motion outliers were further assessed using the FSL Motion Outlier Tool (Jenkinson et al., 2012), which defines outlier thresholds as the 75th percentile plus 1.5 times the interquartile range. TRs identified as outliers were incorporated into the GLM using regressor-based censoring. If greater than 15% of TRs that compose a trial are outliers, the trial was excluded from analyses. One subject was excluded according to this standard. Head motion was generally ideal, with 99.8% of all analyzed TRs (98.1% including the excluded subject) falling within an acceptable range.

The final stage of fMRI preprocessing involved spatial smoothing, spike regression, nuisance variable removal, and optional parcellation-based signal extraction. This process was adapted from the nltools naturalistic analysis pipeline [v0.4.7] developed by Luke Chang and colleagues (2018). For each run, preprocessed functional images (in MNI152NLin2009cAsym space) were loaded and smoothed using a 6mm full-width at half maximum (FWHM) Gaussian kernel to increase signal-to-noise ratio while preserving spatial specificity. Global and differential intensity spikes were identified using a cutoff of 3 standard deviations from the global mean signal, and spike regressors were generated to model and remove their influence. Motion confounds were derived from fMRIPrep outputs and included the six rigid-body realignment parameters (translations and rotations), their first derivatives, and squared terms. These were z-scored and expanded into a design matrix, which was combined with cerebrospinal fluid (CSF) signals and polynomial drift terms (linear and quadratic) to create a comprehensive nuisance model. This design matrix was regressed from the smoothed functional data, and the residuals were retained for subsequent analyses. It should be noted that MVPA analyses like ISC, which are sensitive to the voxel-level patterns that spatial smoothing could distort, are robust to the standard gaussian kernel size that fMRIPrep applies during spatial smoothing (Hendriks et al., 2017). This rigorous denoising pipeline was applied consistently across both social (e.g., uncertainty-related) and non-social tasks to ensure comparability and optimize data quality for individual- and group-level modeling.

Anatomical Parcellation. Functional data were parcellated into a functionally-defined region-of-interest schema (n_{roi} = 100) using the 2022 17-network Schaefer-Kong Atlas (Schaefer et al., 2018). I selected the Schaefer cortical parcellation atlas (Schaefer et al., 2018) because: 1) its functional basis makes it well-suited for capturing distributed functional organization in task-based fMRI, 2) its convolution with network approaches which facilitates network-level analyses, and 3) the atlas has been extensively validated and widely used across studies, enhancing the comparability and reproducibility of findings within the field. While the Schaefer-Kong Atlas is available in resolutions from 100 to 1000 parcels, the 100-region schema was chosen because it provides improved signal-to-noise ratio, relative to higher resolution schemas, by averaging over larger cortical areas, yielding more reliable estimates of regional activity, which is particularly important for naturalistic fMRI data and between-subject analyses. Additionally, this resolution reduces the computational burden and multiple comparisons inherent in region-by-region analyses while aligning well with canonical large-scale functional networks.

Important Recurring Concepts and Computational Definitions

All data analyses noted were conducted in R (v4.4.0) (R Core Team, 2022) via Posit's RStudio (Build 353) using the Ubuntu operating system (20.04.4 LTS). The Tidyverse suite of tools (Wickham et al., 2019) was used extensively for convenient data wrangling. All other relevant libraries are mentioned below when pertinent.

Appraisal Engagement. To identify participants who were disengaged or responded erratically during continuous appraisal tasks, I computed the variance of the standardized first derivative of each subject's rating time course. This is computed by finding the rating difference between successive time points (i.e., the first derivative), z-standardizing the difference within, and calculating the variance of this standardized derivative vector. This approach was selected over traditional measures of raw variance because it captures the temporal dynamics of responding rather than static variability. For instance, a participant who uses the full scale but only shifts their rating once (e.g., jumping from −100 to +100 midway through the video) may exhibit high overall variance despite being functionally disengaged. In contrast, the first derivative reflects the rate and direction of moment-to-moment updates, providing a clearer signal of dynamic engagement with the stimulus. Standardizing the derivative further accounts for individual differences in scale usage, enabling fairer comparison across participants regardless of their preferred rating range or baseline. As a result, this measure allows us to more accurately flag flat or erratic trajectories that may otherwise confound downstream analyses.

Appraisal Clustering. Appraisal clustering refers to the tendency for individuals who engage with the same naturalistic stimulus to exhibit categorically similar patterns of appraisal, such that their trajectories can be reliably quantitatively grouped into distinct types. To capture this latent structure in participants' time-resolved responses, I employed a k-means clustering pipeline on each subject's z-standardized appraisal time course. Each subject's ratings, whether densely sampled (e.g., every 2 seconds in the neuroimaging study) or sparsely sampled (e.g., 34 points in the sparse sampling study), were treated as a feature vector in a time-aligned matrix. Z-standardization ensured that clustering emphasized the shape and timing of each subject's response rather than differences in scale usage.

For clustering of high-resolution data, I first applied principal components analysis (PCA) to reduce dimensionality while preserving temporal variance. The minimum number of principal components needed to explain 90% of the variance was retained. K-means clustering was then performed on the resulting PCA scores using 200 random initializations to reduce sensitivity to local minima. The k-means algorithm partitions participants into k clusters by minimizing the within-cluster sum of squared distances, with each cluster representing a shared trajectory shape across time. The optimal number of clusters (k) was determined using three complementary techniques: (1) the elbow method with the acceleration heuristic, (2) the elbow method with the maximum curvature heuristic, and (3) average silhouette width.

The elbow method identifies the point at which adding additional clusters yields diminishing returns in explained variance, typically visible as a bend or inflection in the within-cluster sum of squares curve. I implemented two variants of this approach: the acceleration method, which selects the point with the largest second derivative (i.e., where the rate of improvement drops most sharply) (Satopaa et al., 2011), and the max curvature method, which identifies the point with the greatest perpendicular distance from a line drawn between the first and last values on the curve (i.e., the most pronounced geometric "knee") (Zhang et al., 2017). The acceleration method tends to be more permissive, while the max curvature method is more conservative; using both provided a principled range of candidate solutions. The silhouette method, by contrast, selects the number of clusters that maximizes how well each point fits within its assigned cluster relative to other clusters (Rousseeuw, 1987). These approaches were implemented using custom functions the factoextra package (Kassambara & Mundt, 2020). The silhouette-optimal k was selected when it fell within the elbow-determined range; otherwise, the mean of the elbow bounds was used, with a slight correction to counteract banker's rounding artifacts inherent to the structure of rounding in R (*IEEE Standard for Floating-Point Arithmetic*, 2019).

To evaluate clustering robustness, I conducted a 100-fold bootstrap resampling procedure and computed pairwise Adjusted Rand Index (ARI) scores across solutions. The ARI quantifies agreement between clustering assignments while adjusting for chance (range: –1 to 1), with higher values indicating greater solution stability. Although clustering solutions should ideally be robust regardless of condition, I considered the possibility that clusters may be more stable when defined within condition. To address this, I conducted k-means clustering both within condition (i.e., separately for participants who rated different halves of the video) and across conditions (i.e., collapsing across all participants). I planned to prioritize the within-condition solution if the across-condition clustering yielded lower stability, as assessed by ARI values.

Cluster assignments were used in downstream analyses as both a dependent variable, testing whether neural synchrony predicts shared appraisals, and as a covariate to control for shared interpretive stance. As an unsupervised method, appraisal clustering complements model-free approaches like representational similarity analysis (RSA) or inter-subject correlation (ISC) by offering a structured, hypothesis-generative framework for characterizing complex behavioral variation. Because clustering is unsupervised, it preserves natural variation in interpretation without imposing assumptions about the "correct" appraisal path.

Appraisal Synchrony. Appraisal synchrony refers to the temporal alignment of continuous appraisal ratings across participants who are exposed to the same dynamic stimulus. It captures the extent to which individuals update their evaluations in similar ways and at similar times, providing a window into shared cognitive-affective processing during naturalistic experiences. If clustering captures *who* appraises a stimulus similarly across its full duration, synchrony captures *when* those appraisals align over time and *how strongly* they align.

To quantify this synchrony, I computed sliding-window Pearson correlations between all possible subject pairs' time-aligned appraisal vectors. Each subject's preprocessed rating timecourse was z-standardized to emphasize relative temporal fluctuations and minimize the influence of scale usage. Synchrony was then assessed using a Gaussian-tapered sliding window (window size = 60 s, step size = 12 s, $\sigma = 3$), which prioritized central time points within each window while downweighting edge values. These specified values are in line with other applications of this approach within social neuroscience (Chen et al., 2017; Song et al., 2021). This yielded approximately 105 overlapping windows per participant pair. Observations were excluded from the final synchrony matrix when either participant in a pair showed no variance during a window, as these yielded undefined correlation values. All computations were parallelized using the doMC and foreach packages in R to accommodate the scale of the pairwise comparison process.

The use of Pearson correlation was selected based on simulation-based benchmarking. Although behavioral appraisals represent bounded, potentially non-normally distributed data with frequent rating plateaus and non-linear transitions, Pearson correlation proved to be the most sensitive and stable method for recovering true signal similarity under conditions that mirrored my experimental data (e.g., scaling, noise, lag, and plateauing). In a series of 500 simulations using both sine- and random-walk-based trajectories, I compared Pearson, Spearman, and Zero-Inflated Poisson (ZIP) models. While Spearman is robust to non-normality and ZIP accounts for plateaus, Pearson consistently outperformed both in recovering underlying synchrony. Its ability to preserve linear magnitude structure, rather than collapsing data to ordinal ranks (as with Spearman), made it particularly well-suited for detecting fine-grained covariation in shape and scale.

This measure of appraisal synchrony enabled us to capture shared temporal dynamics across participants, supporting downstream analyses of inter-subject similarity in interpretive stance, attentional convergence, or neural alignment. As a continuous, windowed estimate of shared appraisal processing, appraisal synchrony offers a richer and more temporally precise alternative to summary-level metrics or model-free techniques like RSA or non-windowed ISC, which may overlook subtle but informative temporal structure in appraisals. Synchrony measures generally serve as both an indication of neural reliability (i.e., multiple persons exhibit the same behaviors) and a window into interpersonal alignment, revealing how the brain supports normativity, shared meaning, or consensus during real-world experiences (Nastase et al., 2019), which is especially pertinent in the face of uncertainty or ambiguity.

Neural Synchrony. Neural Synchrony refers to the temporal alignment of brain activity patterns across individuals exposed to the same stimulus, reflecting shared processing or interpretation of incoming information. Higher synchrony suggests that participants are engaging similar neural mechanisms at the same moments in time, often linked to common attentional, emotional, or cognitive responses during naturalistic experiences.

To characterize shared neural processing during naturalistic viewing, I computed inter-subject synchrony in BOLD signal fluctuations using a Gaussian-tapered sliding window correlation pipeline, paralleling the approach used for appraisal synchrony. Preprocessed fMRI time series were extracted for each subject and anatomically defined region of interest (ROI). For each ROI, pairwise Pearson correlations were computed between all subject pairs using a sliding window with a default size of 60 seconds, a 12-second step size, and a Gaussian kernel ($\sigma = 3$) to emphasize local temporal structure while downweighting edge effects. This procedure yielded time-resolved synchrony estimates for each dyad across ~105 windows and 100 ROIs. To support computational scalability, the analysis was parallelized using the doMC and foreach packages. BOLD timecourses were read from subject-specific .csv files, merged into multivariate matrices per task and ROI resolution, and stored in long-form dataframes with associated metadata (e.g., ROI label, timepoint, window size, sigma).

Sliding windows are essential when computing correlations of neural activity during extended naturalistic viewing because spontaneous fluctuations in functional brain activity can reduce the reliability of correlations computed over long, uninterrupted time series (Allen et al., 2014). By segmenting the time course into shorter, overlapping windows and applying a tapered weighting function, I preserve meaningful temporal variation while attenuating edge effects and minimizing the influence of non-stationary noise. This approach has been validated in prior ISC paradigms involving naturalistic video stimuli (Song et al., 2021), where it enables more precise detection of dynamic, stimulus-locked patterns of neural alignment. By aligning this analysis with the appraisal synchrony framework, I enabled direct comparisons between behavioral and neural alignment within comparable circumscribed windows of time and across regions.

Stimulus Complexity. To quantify moment-by-moment complexity in both social and non-social video stimuli, I computed Shannon's entropy, a well-established information-theoretic measure of uncertainty based on the distribution of values over time (Shannon, 1948). Entropy increases as the distribution becomes more unpredictable or uniformly spread, reflecting heightened informational complexity. In the context of appraisal data, high entropy signals moments of divergence across participants' interpretations (e.g., mixed certainty about a suspect's guilt), whereas low entropy reflects strong consensus. For perceptual (non-social) stimuli, entropy reflects variability in visual features such as luminance, with high entropy indicating richly varied frames and low entropy indicating perceptual uniformity. Notably, entropy is agnostic to the central tendency or average value of a distribution. Both high and low mean ratings can be associated with either high or low entropy, depending entirely on how dispersed or concentrated the values are. For instance, a timepoint where all participants strongly agree that a character is guilty (e.g., ratings near 90) would exhibit low entropy, just as a timepoint where all agree on innocence (e.g., ratings near 10) would. In contrast, entropy would be high if participants are split across the scale, regardless of the average, because the distribution reflects interpretive conflict or uncertainty, not consensus. Although entropy is often associated with the concept of uncertainty, I use the term "complexity" to reflect the broader applicability of my entropy-based measures across both perceptual and interpretive domains. This choice also avoids potential confusion with participants' explicit uncertainty ratings while acknowledging the close conceptual ties between complexity, uncertainty, and ambiguity.

To compute appraisal complexity, I used the continuous character ratings collected in the sparse hypothesis sampling study. First, all participant ratings were linearly transformed from the original bipolar scale (−100 to +100) to a unipolar scale (0 to 100), such that 0 reflected certainty of innocence and 100 reflected certainty of guilt. I then applied a Gaussian-weighted sliding window entropy function adapted from the DescTools R package (Signorell et al., 2025), which aggregates rating values within a temporally defined window and computes the normalized Shannon entropy across this local distribution. This allowed us to identify moments of increased interpretive demand as a feature of the stimulus (i.e., where group-level consensus breaks down and multiple appraisal hypotheses are actively maintained). Entropy scores were z-standardized to emphasize relative fluctuations across the stimulus timeline.

To compute luminance complexity for my non-social perceptual control task, I applied the same Gaussian-tapered sliding window entropy function to visual features of the video. Frames were extracted from the stimulus at 3 Hz and converted to grayscale images. Each frame's luminance distribution was calculated via pixel-wise intensity histograms, from which entropy was computed based on the probability of each luminance bin. As with appraisal entropy, higher values reflected greater perceptual variability within a given time window.

This shared computational approach enabled alignment of entropy estimates with behavioral and neural synchrony analyses, allowing us to examine how complexity in social and non-social domains relates to group-level alignment. More broadly, stimulus complexity provides a principled and interpretable signal of when and where individuals face competing interpretations or richly layered sensory input; conditions that may drive shared attention, belief updating, and neural coherence during naturalistic viewing.

Informational Weight. Informational Weight refers to the perceived utility of a given moment in advancing or challenging a specific appraisal. In the context of my task, it captures how strongly a participant believes a moment contributes evidence for or against the guilt of a particular character. Informational weight is hypothesis-dependent and directional, anchored to whether incoming information is seen as consistent or inconsistent with a character's presumed role in the narrative. This concept allows us to examine how subjective weighting of events varies across individuals depending on their interpretive stance.

To quantify how informative each moment of the video was perceived to be, relative to a specific character's hypothesized guilt, I computed moment-by-moment averages of participants' continuous ratings using a Gaussian-tapered sliding window approach. For each character, I first aggregated participant ratings (0–100 scale) at each second of the video, then applied a sliding window with a Gaussian-weighted kernel ($\sigma = 3$) centered on each target timepoint. The window was convolved with the time series, prioritizing temporally local structure while gently downweighting surrounding timepoints. The result was a smoothed trajectory reflecting the average perceived informativeness of each moment, separately for each character. These smoothed timecourses were then averaged across characters to yield a global informational weight index used in downstream analyses. This approach allows us to align periods of peak subjective informativeness with changes in neural or behavioral synchrony, offering insight into how interpretive salience shapes shared cognitive responses to complex stimuli.

Statistical Modeling and Analytic Strategy

All correlations were Fisher's Z transformed prior to inclusions in models and the subsequent relevant estimates (e.g., beta, standard error, etc.) were reversed transformed for interpretation.

Binary Logistic Regression. Binary logistic regressions were implemented in base R to test the relationship between cluster membership (i.e., perspective) and neural synchrony. Separate models were estimated for each ROI, and false discovery rate was controlled using the Benjamini-Hochberg procedure.

Linear Models. Linear regression models were also conducted in base R to assess differences in average appraisal synchrony by cluster type (i.e., intra-cluster synchrony vs. inter-cluster synchrony). Additional models expounded upon this by exploring the predictive utility of the interaction between information complexities and cluster type towards average appraisal synchrony, as well as appraisal engagement and average appraisal synchrony at moments throughout the stimulus.

Hierarchical Linear Modeling. Hierarchical linear modeling, conducted using lme4 (Bates et al., 2015), were fitted for all appraisal-neural synchrony models and employed an information criterion approach for model testing comparing BIC values between competing models. All models began with a null consisting of appraisal synchrony as the criterion and subject pair specified as a random intercept. Models were then constructed iteratively without restricted maximum likelihood to facilitate model comparison. The first model introduced neural synchrony as a fixed predictor of appraisal synchrony, but this model was outperformed (i.e., $p < 0.05$ after correction for multiple comparisons) in all ROIs by Model 2, which specified a random intercept of time. Models 3 and 4 introduced a fixed effect of domain and an interaction between domain and neural synchrony, which again outperformed previously models in nearly every ROI. Finally, Models 5,6 and 7 introduced complexity as a fixed effect, an interaction with neural synchrony, and a three-way interaction among domain and neural synchrony.

Intersubject Correlations. ISC was conducted in base R using pairwise pearson correlations applied to neural values. Significance was determined via permutation testing using 500,000 permutations per ROI.

Correction for Multiple Comparisons. To correct for multiple comparisons in neural analyses, I applied the Benjamini-Hochberg (BH) procedure to control the false discovery rate (FDR) across all parcels. Unless otherwise specified, results were thresholded at a corrected p-value of < .01, ensuring a stringent yet interpretable balance between sensitivity and Type I error control.

Open Access Statement. A detailed outline and scripts associated with pre-processing, analyses, and visualizations are publicly available at and https://github.com/wj-mitchell/dissertation.

CHAPTER 3

RESULTS

Appraisal Clustering Reflects Diverging Perspectives

To identify shared patterns in belief trajectories, I first applied PCA to the z-standardized continuous rating data. When clustering was conducted across all participants, a minimum of 7 principal components was required to explain at least 90% of the variance, compared to 6 and 5 components when PCA was performed separately within Condition A and Condition B, respectively.

In Condition A, the elbow method suggested an optimal k range of 2–3, while the silhouette method favored k = 2. Clustering with k = 2 yielded a highly stable solution (median ARI = 1.00, SD = 0.24, min = –0.50, max = 1.00, n = 4,949), with an approximately even split of 11 and 9 subjects across the two clusters. These clusters captured diverging belief trajectories: one group (Cluster 1) became increasingly certain that Jonathan was guilty, while the other (Cluster 2) became increasingly confident in his innocence. These trends can be observed in **Figure 4**.

In Condition B, the elbow method indicated an optimal k of 3, while the silhouette method again favored k = 2. Clustering produced a similarly stable solution (median ARI = 1.00, SD = 0.34, min = –0.50, max = 1.00, n = 4,910), resulting in three clusters with 5 subjects each. Two of the clusters mirrored the patterns observed in Condition A (rising certainty of guilt vs. innocence), while the third remained centered near the midpoint of the scale, suggesting persistent uncertainty across the stimulus.

When collapsing across conditions, the elbow method supported k = 3, while the silhouette method again suggested k = 2. The clustering solution across all subjects yielded the most stable ARI profile (median = 1.00, SD = 0.23, min = –0.08, max = 1.00, n = 4,950) and produced two clusters of 16 and 19 subjects, respectively. Given its superior stability and my pre-specified plan to use the across-condition solution when reliable, I retained this final clustering structure for downstream analyses.

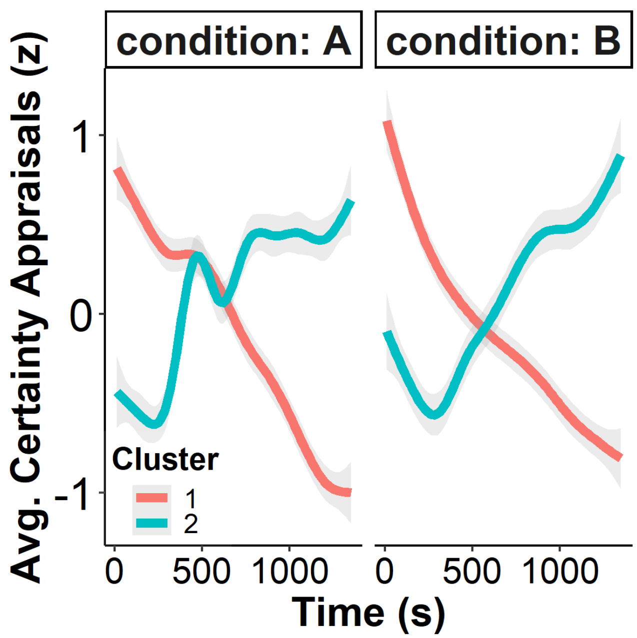

Figure 4. Appraisal Cluster Trajectories Using Generalized Additive Models with a cubic regression spline basis, we visualized average appraisal rating trajectories over time for each cluster during the first and second (i.e., conditions A & B, respectively) stimulus videos. All values were within-subject standardized. Positive z-values trend toward greater certainty of the target character's innocence. Negative z-values trend towards greater certainty of the target character's guilt. Shaded regions denote 95% confidence intervals.

Having identified stable clusters that reflected diverging interpretations, I next asked whether these global patterns of appraisal also manifested as greater moment-to-moment alignment between individuals within the same cluster, testing whether shared interpretive frames extend beyond overall trajectories to shape real-time evaluative behavior.

Shared Perspective Enhance Appraisal Synchrony

To evaluate whether cluster membership predicted greater alignment in moment-by-moment behavioral judgments, I regressed appraisal synchrony onto a binary indicator of cluster type (intra-cluster vs. inter-cluster). Analyses were conducted separately using both the mean and median correlation within each window to ensure robustness against potential outliers or skew. In both models, intra-cluster pairs exhibited significantly greater synchrony than inter-cluster pairs. When using mean correlation as the outcome, intra-cluster pairs were associated with a large increase in synchrony (b = 0.46, $t(255)$ = 11.99, error = 0.04, $p < .001$), accounting for 36.0% of the variance (R^2 = 0.36). A nearly identical pattern emerged when using median correlation (b = 0.54, $t(255)$ = 11.23, std. error = 0.05, $p < .001$), with the model explaining 33.1% of the variance. These results confirm that clustering based on participants' overall rating trajectories captures meaningful behavioral similarity: participants with similar interpretive orientations to the stimulus tended to respond in more synchronized ways throughout viewing.

While these findings demonstrate that shared interpretive frames support greater alignment in appraisal behavior, they leave open the question of how features of the stimulus itself - particularly its moment-to-moment informational complexity - might amplify or constrain this synchrony.

Appraisal Complexity Amplifies Shared Perspective

I next examined whether appraisal complexity moderates the relationship between appraisal clustering and moment-to-moment synchrony, under the hypothesis that ambiguous moments would amplify reliance on shared interpretative frameworks and thus increase intra-cluster appraisal synchrony.

individuals within the same cluster may interpret ambiguous moments more similarly by drawing on their shared interpretative frameworks. A linear model revealed a

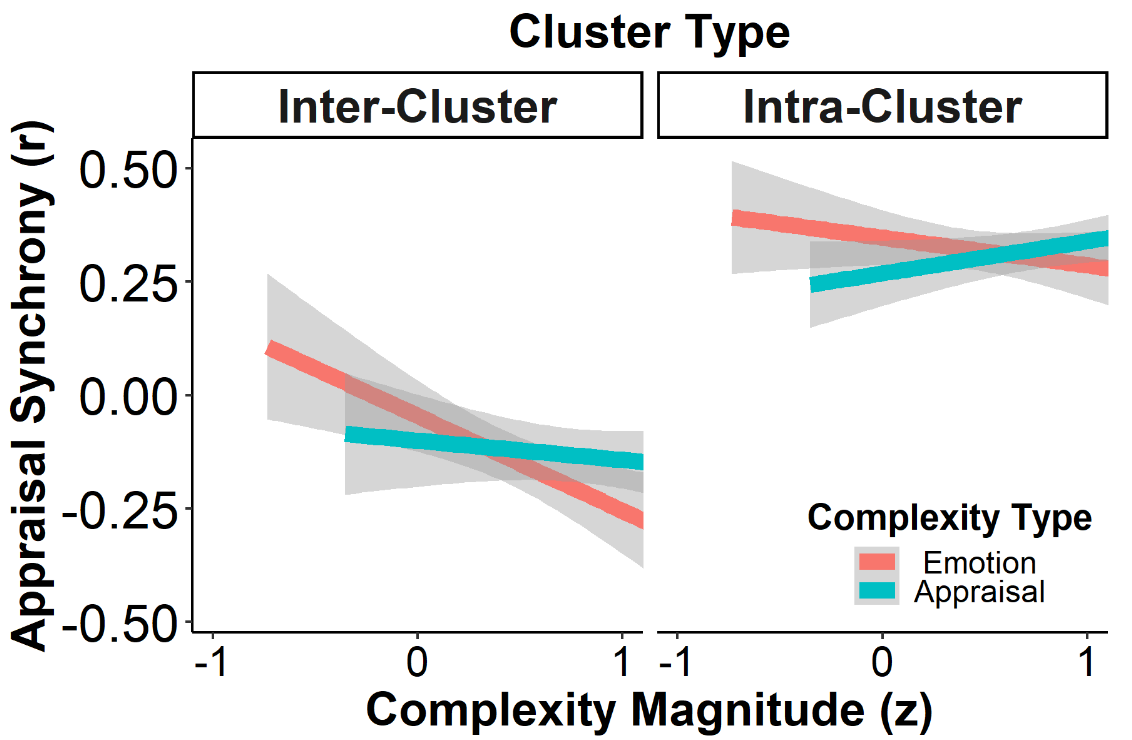

Figure 5. The Effects of Complexities Upon Appraisal Synchrony By Perspective Linear models revealed marginally significant interactions between complexity type and cluster membership. Appraisal complexity was associated with increased synchrony among individuals within the same appraisal cluster, but reduced synchrony between clusters. Emotional complexity showed a general negative association with appraisal synchrony, though this effect was attenuated for intra-cluster pairs.

marginally significant interaction between cluster type (i.e., inter-cluster vs. intra-cluster comparisons) and appraisal complexity (b = 0.13, $t(256)$ = 1.86, std. error = 0.07, p = .064, R^2 = 0.37) (**Figure 5**). This is consistent with the idea that shared cognitive framing may scaffold appraisal alignment particularly when uncertainty is high, though, caution is warranted in interpreting any marginally significant effects. Furthermore, I find no evidence to suggest that appraisal complexity synchronizes appraisals generally, or without taking perspectives into account (b = 0.00, $t(258)$ = 0.084, std. error = 0.04, p = 0.93, R^2 = 0.00) (**Figure 6**). These findings suggest that complexity can enhance appraisal alignment within perspective, but they leave open the question of whether this effect reflects a general property of complexity or is specific to moments of interpretive ambiguity. To test this, I examined whether emotional complexity, which is another form of informational variability, exerts a similar influence on appraisal synchrony.

Emotional Complexity Reduces Appraisal Synchrony

I repeated the same analysis using "emotional complexity" as a predictor. This measure was derived from the output of *EmoNet*, a deep neural network trained to identify discrete emotional expressions in visual stimuli (Kragel et al., 2019). For each still frame of the stimulus, EmoNet produced probability estimates across twenty discrete emotion categories (i.e., the probability that each emotion was represented within the still frame), which were then used to calculate the average Shannon's entropy value within each window using the same method outlined for appraisal complexity.

Emotional complexity, unlike appraisal complexity, demonstrated a negative effect upon appraisal synchrony independent of cluster type (b = -0.134, t(258) = -2.54, std. error = 0.05, $p < 0.05$, $R^2 = 0.02$), such that moments of higher emotional ambiguity yielded less appraisal synchrony overall (**Figure 6**). Emotional complexity also unfortunately only yielded a marginally significant interaction with cluster type (b = 0.14, t(256) = 1.77, std. error = 0.08, $p = 0.077$, $R^2 = 0.36$), which may suggest that intra-cluster appraisal synchrony is less negatively impacted by emotional complexity than inter-cluster appraisal synchrony (**Figure 5**). However, a linear model exploring the interaction between complexity type and complexity magnitude did reveal a significant interaction effect (b = 0.14, t(516) = 2.047, std. error = 0.07, $p < 0.05$, $R^2 = 0.01$), indicating that emotional and appraisal complexity do exert differing effects on appraisal synchrony.

Taken together, these findings suggest that informational complexity does not promote universal alignment but instead strengthens coherence within shared perspectives. While appraisal complexity enhanced synchrony among individuals with similar interpretive frames, emotional complexity broadly disrupted synchrony. However, these effects raised the question whether complexity truly represents alignment in appraisal changes or could simply results from broad disengagement.

Figure 6. The Effects of Complexities Upon Appraisal Synchrony Linear models found no relationship between appraisal complexity and appraisal synchrony, but revealed a negative association between emotional complexity and appraisal synchrony. A significant interaction between complexity type and entropy magnitude confirmed that appraisal and emotional complexity exert statistically distinct effects on synchrony.

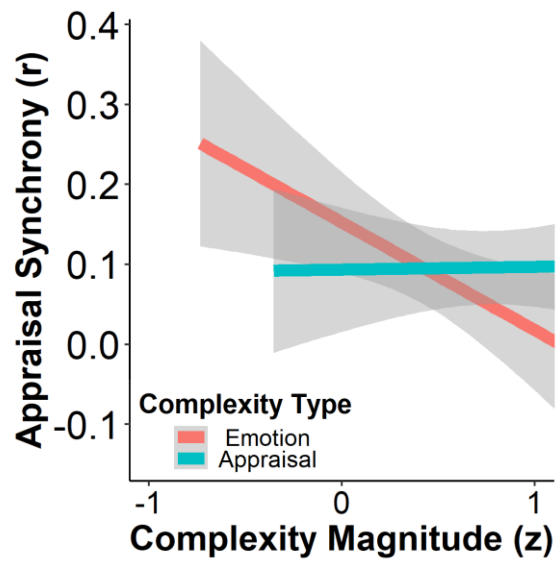

Appraisal Synchrony Reflects Cognitive Engagement, Not Inactivity

To ensure that observed increases in cluster synchrony were not merely artifacts of shared plateaus or minimal rating change (i.e., low temporal signal), I tested whether the average appraisal engagement predicted appraisal synchrony. Linear models revealed that mean cluster synchrony was strongly and positively associated with appraisal engagement ($b = 0.88$, $t(258) = 36.72$, std. error = 0.02, $p < .001$, $R^2 = 0.84$). This result suggests that moments of high synchrony were not characterized by flat or plateaued ratings, but rather by increased dynamic alignment in rating trajectories, supporting the interpretation that synchrony reflects meaningful temporal coherence rather than shared inactivity.

Having established that appraisal synchrony reflects genuine cognitive engagement and that such synchrony increases within perspectives during appraisal-complex moments, I next asked whether the inverse might also be true: do moments of high informational clarity, or *informativeness*, promote convergence even across divergent perspectives? Since informativeness reflects the presence of clear, diagnostic cues, it should theoretically oppose ambiguity and foster alignment between clusters rather than within them. I tested this possibility by examining the relationship between perceived informativeness and cluster-specific appraisal synchrony.

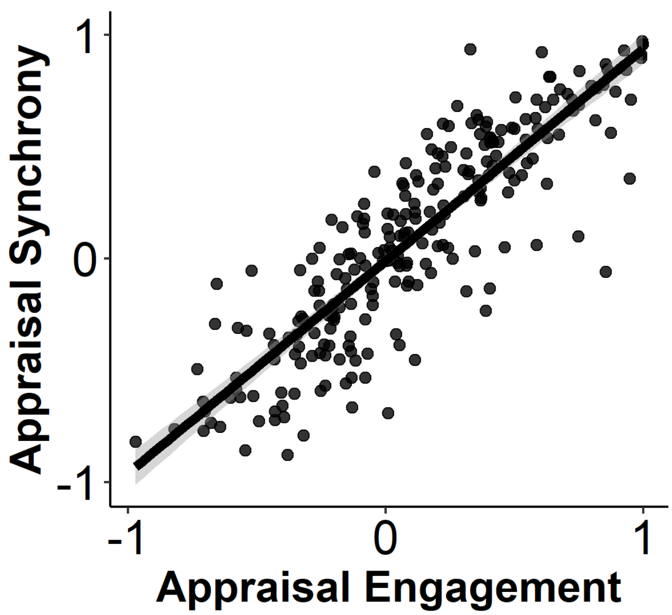

Figure 7. Appraisal Engagement Predicts Synchrony To rule out the possibility that synchrony was driven by shared plateaus in appraisal ratings, we tested whether synchrony was associated with dynamic engagement (i.e., variability in rating changes over time). A linear model revealed a strong positive relationship between appraisal synchrony and engagement, indicating that synchrony reflects active alignment rather than inactivity.

Informational Weight Synchronizes Appraisals Regardless of Perspective

Consistent with prior expectations, informativeness was strongly and negatively correlated with appraisal complexity (r = –0.64), suggesting that scenes perceived as more informative were also those in which character evaluations became more constrained and less ambiguous across viewers. Information weight significantly interacts with appraisal cluster type (b = -0.01, t(256) = -1.99, std. error = 0.01, $p < 0.05$, R^2 = .37) such that intra-cluster appraisal synchrony decreases as information weight increases, and inter-cluster appraisal synchrony demonstrates a positive relationship. This interaction relationship is further amplified if specifically focusing upon the informational weight of Jonathan Fraser's character (b = -0.01, t(256) = -3.556, std. error < 0.01, $p < 0.001$, R^2 = .41) This suggests that the scenes rated as most diagnostic about his involvement may have prompted more uniform reactions even across individuals with opposing interpretations.

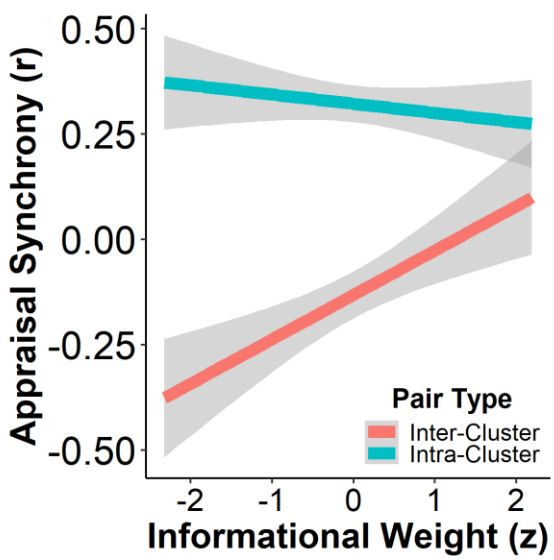

Figure 8. Informational Weight – Cluster Type Predicts Appraisal Synchrony A linear model found that informational weight yields effects in opposite of appraisal complexity: inter-cluster appraisal synchrony increases as informational weight increases, while intra-cluster appraisal synchrony decreases. This may reflect the effects of a "clear signal" leaving little opportunity for interpretative framework influence.

Shared Perspectives Cannot Be Inferred from Neural Synchrony Alone

Having identified distinct behavioral clusters and shown that moment-to-moment appraisal synchrony is shaped by shared interpretations and stimulus complexity, I next asked whether these interpretive alignments were mirrored at the neural level. Specifically, I tested whether inter-subject neural synchrony predicted membership in the same appraisal cluster, linking shared cognition to shared brain dynamics. To evaluate whether intersubject neural synchrony predicted behavioral clustering, I conducted a series of binary logistic regressions; one for each parcel in the 2022 Schaefer 100-parcel, 17-network parcellation (Schaefer et al., 2018). Prior to correction for multiple comparisons, five regions met conventional significance thresholds ($p < .05$). Three regions showed positive associations, indicating that greater neural synchrony was associated with an increased likelihood of belonging to the same behavioral cluster: the right inferior parietal lobule (ROI 77; OR = 18.17, std. error = 1.12, $p = .009$), the right parahippocampal cortex (ROI 58; OR = 15.04, std. error = 1.16, $p = .020$), and the left superior parietal lobule (ROI 31; OR = 13.87, std. error = 1.18, $p = .026$). These parcels fall within the ventral attention, default mode, and dorsal attention networks, and may reflect distributed functional systems supporting shared behavioral trajectories during naturalistic viewing. However, none of the models survived false discovery rate correction (adjusted $p \geq .635$), and these findings should therefore be interpreted cautiously pending replication in future work.

Social and Non-Social Appraisals Broadly Synchronize Brain Networks

To identify brain regions exhibiting robust inter-subject synchronization during naturalistic decision-making, I computed ISC separately for social and non-social conditions across all 100 cortical parcels and tested each against a null distribution using permutation-based significance testing with Benjamini–Hochberg correction (n = 500,000).

Significant synchronization was widespread, with 92 out of 100 regions surpassing a threshold of $p < .01$. While robust ISC was observed in visual A (*avg.* $r = 0.25$) and auditory networks (*avg.* $r = 0.36$) as expected, several higher-order association networks also showed strong alignment. Notably, parcels within the default mode networks A (*avg.*

r = 0.08) and C (*avg.* r = 0.12), dorsal attention network A (*avg.* r = 0.09), and salience/ventral attention network B (*avg.* r = 0.07) demonstrated among the highest non-sensory ISC values, suggesting that shared interpretation and attentional allocation contributed to convergent neural activity during naturalistic social processing. Notably synchronized higher-order regions include the right temporal pole, parietal occipital lobe, precuneus, parahippocampal cortex, and superior parietal lobe, all of which demonstrated a synchrony value of 0.1 or higher.

In the non-social model, 69 out of the 100 regions demonstrated significant inter-subject synchronization at a threshold of $p < .01$. These effects were broadly distributed, but several networks exhibited especially consistent synchronization. Notably, the Dorsal Attention (A & B) (*avg.* r = 0.05), Visual (A–C) (*avg r's* = 0.09 – 0.17), and Default Mode (particularly Default C) (*avg.* r = 0.07) networks each contributed six or more significant regions. The most synchronized non-sensory ROIs included regions within dorsal attention and control networks, reinforcing the role of top-down attentional systems in structuring neural synchrony during non-social processing. Values for all parcellations are contained within the master synchrony results table in the appendix.

Social Appraisals Drive Greater Neural Synchrony Than Non-Social

Directly comparing the two conditions revealed 56 parcels where ISC was significantly higher during social versus non-social tasks. These included bilateral medial and lateral prefrontal cortices, bilateral posterior cingulate, and several left-lateralized dorsal attention and ventral attention network parcels, including the superior and inferior parietal lobe. No parcels showed significantly greater ISC during non-social compared to social tasks (**Figure 9**). The largest higher-order network differences were observed in

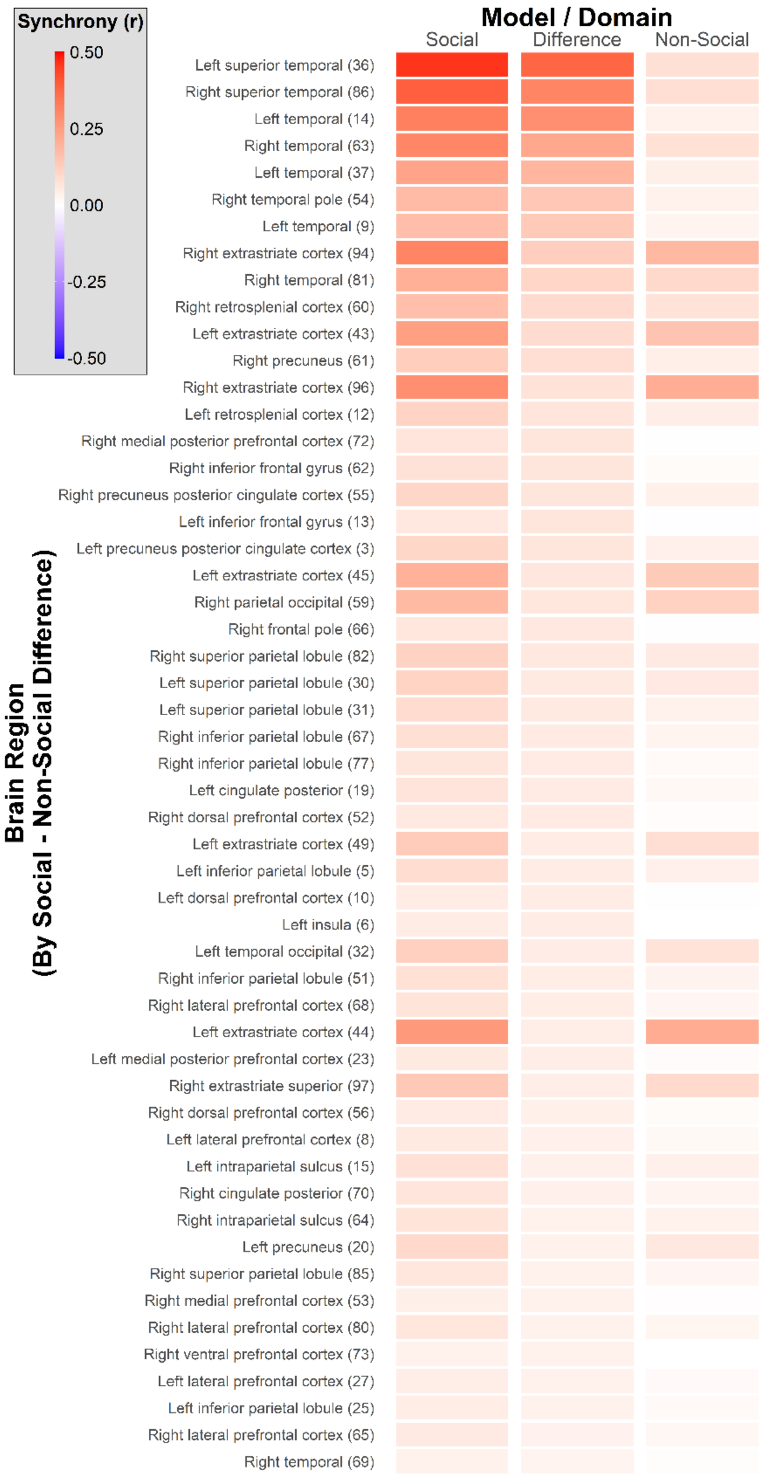

Figure 9. Domain-Specific Intersubject Correlation Values By Region Intersubject correlations were computed across 100 cortical parcels from the Schaefer 2022 parcellation, separately for social and non-social tasks, as well as for their difference (Social – Non-Social). Each row corresponds to a brain region, labeled by hemisphere, anatomical name, and parcellation index, and sorted in descending order of difference-score magnitude. Color saturation reflects the correlation coefficient (r) for each region and condition. Warmer difference colors (center panel) indicate greater intersubject synchrony during social appraisals relative to non-social tasks. Significance was assessed using permutation testing (n = 500,000) within each region and corrected for multiple comparisons using the Benjamini–Hochberg procedure to control the False Discovery Rate (FDR). Only regions which demonstrated $p < 0.01$ in the difference model are visualized.

default mode networks A, B, and C (*avg. r's* = 0.05). These results may collectively indicate that naturalistic social inference tasks elicit more widespread and consistent cortical synchrony than non-social tasks, especially in midline and temporoparietal regions commonly implicated in theory of mind, narrative comprehension, and attentional reorienting, but some differences in task design may limit this interpretation. See **Table 1** for a full list of ISC network results.

Network	Difference (avg. *r*)	Non-Social (avg. *r*)	Social (avg. *r*)
Auditory	0.293	0.069	0.363
Control (A)	0.033	0.027	0.059
Control (B)	0.034	0.012	0.047
Control (C)	0.039	0.018	0.057
Default (A)	0.054	0.024	0.078
Default (B)	0.051	0.016	0.066
Default (C)	0.055	0.070	0.125
Dorsal Attn (A)	0.037	0.049	0.086
Dorsal Attn (B)	0.007	0.039	0.046
Language	0.161	0.030	0.191
Sal / Ventral Attn (A)	0.012	0.028	0.041
Sal / Ventral. Attn (B)	0.039	0.031	0.070
SomatoMotor (A)	-0.006	0.034	0.029
SomatoMotor (B)	0.026	0.021	0.046
Visual (A)	0.072	0.175	0.247
Visual (B)	0.021	0.092	0.113
Visual (C)	0.037	0.091	0.128

Table 1. Average Network Synchrony By ISC Analysis Networks correspond to the 2022 17-Network Kong schema and each value represents the average ISC value across all Schaefer parcellations. contained within that network. Negative values are colored red.

Neural Synchrony Predicts Social and Non-Social Appraisal Synchrony

To examine whether neural synchrony predicted social appraisal synchrony, I tested mixed-effects linear models with a random intercept for dyad and timepoint. Only two non-motor regions, the left lateral PFC within Control Network A and the left insula, achieved significance at my target threshold, demonstrating positive and negative connectivity, respectively. Additional regions achieved significance at a threshold of $p < 0.05$, including regions in the default mode (left temporal pole), control (left temporal lobe, right lateral PFC), salience/ventral attention (bilateral insulae, right IPL), somatomotor (right insula), dorsal attention (right SPL, right posterior cingulate), and visual networks. The right lateral PFC and right SPL were the only regions to demonstrate a positive association; all others yielded negative estimates.

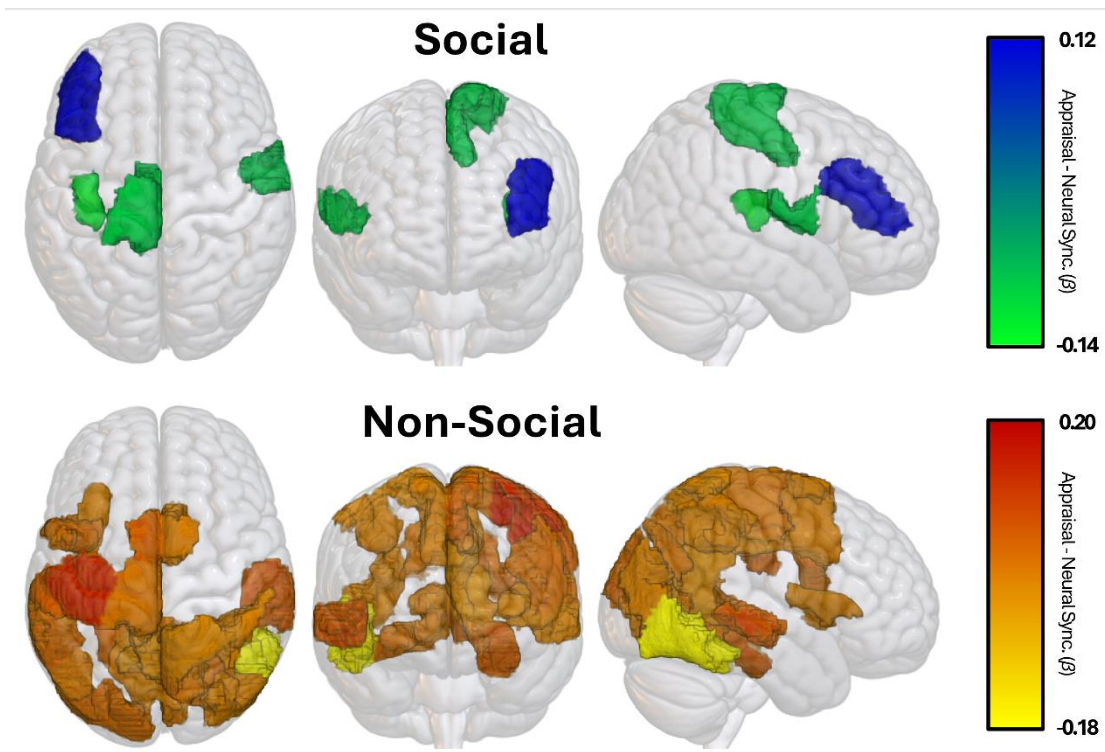

Figure 10. Domain-Specific Appraisal-Neural Synchrony Associations Hierarchical linear models identified several regions that synchronized or de-synchronized as social or non-social appraisals synchronized. Among social appraisals, the left lateral PFC synchronized while the right insula and left motor regions desynchronized. Among non-social appraisals, we see a broader constellation of primarily posteriorly-located sensory regions which demonstrated moderate synchronization overall.. All regions visualized achieved an adjusted $p < 0.01$.

In contrast, a robust constellation of regions demonstrated significant positive connectivity during the non-social task. These included bilateral superior parietal lobes, bilateral striate and extrastriate, medial prefrontal cortex, bilateral precuneus, bilateral frontomedial lobe, the left insula, the right intraparietal sulcus, bilateral temporal lobe, and the left inferior parietal lobe. Notably, even when operating at the liberal threshold of $p < 0.05$, the only regions activated by both domains are the left extrastriate, left somatomotor area, and right SPL in the dorsal attention network (**Figure 10**).

A model specifying task as an interaction with neural synchrony revealed that the right lateral PFC did preferentially activate for social appraisals, while bilateral IPLs, left insula, visual network structures, left SPL, right IPL, and left temporal lobe preferentially activated for the non-social condition (**Table 2** in **Appendix**).

These findings suggest that moment-to-moment alignment in appraisals may be more tightly scaffolded by regional neural synchrony during perceptually driven, lower-order tasks than during complex, socially evaluative decision-making, where broader or more variable cognitive processes may dominate.

Social Neural–Appraisal Synchrony Improves Within Perspective

Building from previous results, I explored whether appraisal-neural synchrony strength would be improved by accounting for perspective, so an additional model including a cluster-neural synchrony interaction and using only social observations was specified. It otherwise mirrored the previously noted social model. This revealed several regions which appear to synchronize more when subjects share perspectives (**Figure 11**). Regions which appear to synchronize more when subjects share a perspective showing include the right lateral prefrontal cortex in Control Network A, the right middle prefrontal cortex in Control Network C, the right lateral prefrontal cortex in the Salience/Ventral Attention Network B, the left posterior cingulate in Control Network C, and the left frontal pole within the Default Mode Network B.

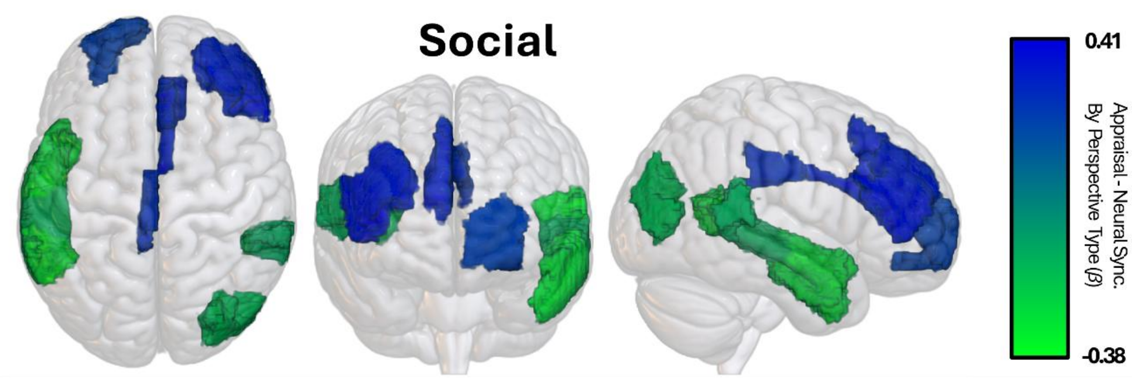

Figure 11. Perspective-Sensitive Social Appraisal-Neural Synchrony Hierarchical linear models identified several regions that synchronize more or less when subjects share perspectives. A general trend appears to suggest that higher-order frontal circuitry synchronizes more while individuals entertain similar perspectives in social appraises, while some sensory regions desynchronize. All regions visualized achieved an adjusted $p < 0.01$.

In contrast, regions which appear to desynchronize when subjects share perspective were predominantly observed in temporal and visual cortices. These included the left auditory temporal region, the left temporal region of the Default Mode Network B, the right extrastriate visual cortex, the left temporal cortex of the Language Network, and the right temporal cortex of the Salience/Ventral Attention Network B. All results are summarized in **Table 3** in the **Appendix**. Together, this pattern may reflect a functional shift away from sensory and perceptual processing toward higher-order cognitive appraisal or interpretive engagement, depending on the demands or content of the stimulus and whether individuals are tracking similar conclusions.

Neural–Appraisal Synchrony Varies by Complexity Across Regions

Next, I explored which regions were sensitive to complexity via interaction with neural synchrony while adjusting for domain. These included regions within the default mode network (e.g., left insula, right parieto-occipital cortex), dorsal attention network (left SPL, left temporo-occipital cortex), salience/ventral attention network (right lateral PFC, right temporal lobe), language network (bilateral temporal lobe), control networks (left precuneus, right lateral PFC), and visual areas, highlighting a core set of task-general systems in which complexity dynamically modulates the behavioral relevance of shared neural activity, regardless of whether the appraisal is occurring in the social or non-social domain.

Perspective and Complexity Co-Construct Appraisal-Neural Synchrony

Lastly, I explored how domain further colored this relationship. A hierarchical linear model examining the three-way interaction between neural synchrony, task domain (social vs. non-social), and complexity revealed a distributed set of brain regions in which higher neural synchrony was more predictive of appraisal synchrony specifically during high-complexity moments, and this relationship was moderated by task domain. Significant positive three-way interactions were observed in several default mode network (DMN) regions, including the right temporal pole, left temporal pole, bilateral dorsomedial prefrontal cortex, and left posterior dorsomedial prefrontal cortex. In addition, the left inferior parietal lobule and bilateral superior parietal lobule within the salience and ventral attention network were involved, along with the right superior temporal gyrus (auditory cortex) and right postcentral gyrus (somatomotor cortex). Visual cortex contributions included the left extrastriate cortex, left striate cortex, and right extrastriate cortex. These findings suggest that moments of high informational complexity may recruit both higher-order association and lower-level sensory regions to facilitate shared appraisal, contingent on social framing.

When examining the non-social condition in isolation, significant positive complexity-by-synchrony interactions were observed in visual regions such as the left extrastriate cortex, left superior extrastriate cortex, and left striate cortex, as well as the left temporal cortex (language area) and left precentral gyrus (dorsal attention network). Notably, the right inferior parietal lobule within the salience network showed a significant negative interaction, indicating that greater synchrony in this region may reduce alignment of appraisals under complex non-social conditions (**Figure 12**).

For the social condition, positive interaction effects were widespread and included visual areas such as the left and right extrastriate cortex and left extrastriate area 3, right temporal cortex (language area), and regions throughout the default mode network, including the right and left temporal pole, bilateral dorsomedial prefrontal cortex, right inferior parietal lobule, left posterior cingulate/precuneus, left posterior insula, and right parahippocampal cortex. Additional effects were observed in the right and left superior parietal lobule, left temporo-occipital cortex, and left posterior cingulate, as well as control network regions in the right prefrontal cortex and left precuneus. Right frontal medial cortex and right superior extrastriate cortex within the salience network were also implicated.

The significance of this three-way interaction indicates that the relationship between neural synchrony and appraisal synchrony is not static, but rather depends on both the degree of stimulus complexity and the social context of the task. That is, neural alignment among individuals is most predictive of shared interpretation during ambiguous moments, and this predictive power is further shaped by whether participants are attending to social or non-social aspects of the stimulus. This pattern highlights the flexible, context-sensitive nature of social appraisal alignment and its grounding in coordinated neural dynamics.

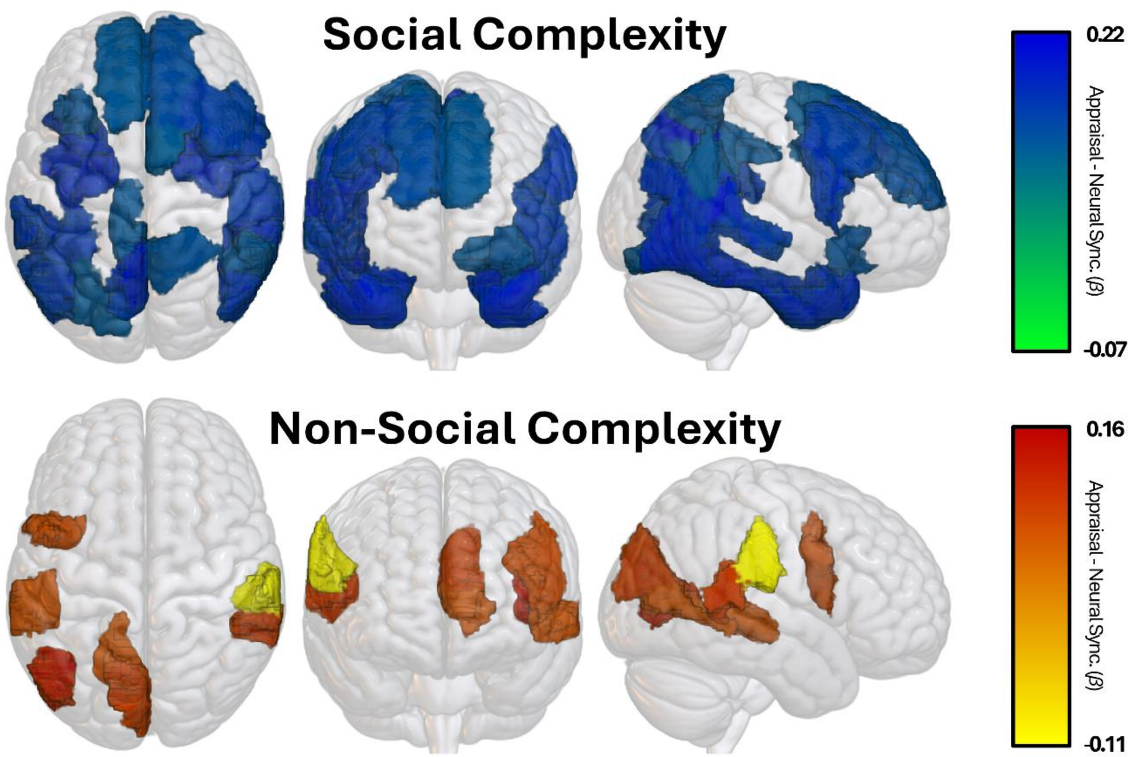

Figure 12. Complexity-Sensitive Appraisal-Neural Synchrony By Domain Complexity appeared to moderate the appraisal-neural synchrony association in some sensory regions, while complexity affected a much broader constellation of regions across default mode, attention, and control networks within the social domain. All regions visualized achieved an adjusted $p < 0.01$.

CHAPTER 4

DISCUSSION

This dissertation aimed to characterize the neural circuitry that normatively supports the formation of explicit appraisals in response to both social and non-social sources of uncertainty. By leveraging temporally resolved naturalistic stimuli and dynamic modeling approaches, the goal was to trace how distributed patterns of neural activity give rise to evolving judgments under dynamic and complex conditions. A secondary aim was to examine how both internal factors (e.g., shared interpretive perspective) and external factors (e.g., moment-to-moment stimulus complexity and informational weight) modulate the strength and reliability of this brain–behavior relationship. In doing so, this work sought to clarify when and where neural synchrony predicts convergent appraisals, and how contextual variability alters this mapping across cognitive domains.

Several core findings emerged. First, participants formed distinct interpretive trajectories when resolving uncertainty, with stable clusters emerging across independent subsamples. These shared perspectives were behaviorally meaningful: individuals within the same cluster showed significantly greater alignment in moment-to-moment appraisals than those across clusters. Second, appraisal synchrony was modulated by the complexity of the stimulus. Moments of high appraisal complexity amplified intra-cluster synchrony, consistent with the hypothesis that individuals lean more heavily on shared interpretive frames when ambiguity is high. In contrast, emotional complexity broadly reduced synchrony, likely due to greater variance in affective interpretation. Importantly, these effects could not be attributed to disengagement or plateauing, as synchrony was positively associated with dynamic appraisal engagement.

Third, stimulus informativeness - particularly information implicating the suspect - promoted convergence even across divergent interpretive clusters, suggesting that diagnostic cues can temporarily override top-down biases and facilitate shared evaluation. Fourth, widespread neural synchrony was observed across participants, with frontal and midline regions, including medial prefrontal, posterior cingulate, and lateral parietal areas, more strongly synchronized during social versus non-social appraisal. Conversely, dorsal attention and sensory networks were more synchronized during non-social processing, consistent with task demands.

Fifth, neural synchrony predicted appraisal synchrony across both domains, but the spatial distribution of effects diverged. Social appraisals were scaffolded by default mode and control regions, while non-social appraisals were supported by parietal and visual networks. Sixth, perspective and complexity jointly modulated the strength of brain–behavior coupling. Several higher-order association areas - including dorsomedial PFC and bilateral temporal poles - demonstrated stronger neural–appraisal alignment among individuals with shared perspectives, particularly during complex moments. Finally, a significant three-way interaction between neural synchrony, domain, and complexity revealed that the predictive relationship between brain and behavior was strongest when appraising ambiguous social information.

Together, these findings offer a comprehensive account of how shared interpretations emerge in naturalistic contexts and demonstrate that synchronized social understanding is grounded in dynamic, context-sensitive neural mechanisms. These findings likely speak to at least a few related literatures which I will briefly review.

Confirmation Bias and Heuristics

Participants who initially shared the same suspicion about the character's guilt became increasingly aligned in their certainty as the episode progressed. Rather than shifting perspectives, most participants became more confident in their original interpretation, particularly during moments of high ambiguity. This pattern may suggest a potential tendency to selectively integrate evidence that supported pre-existing beliefs akin to confirmation biases. Prior work has shown that individuals often interpret ambiguous information in belief-consistent ways, leading to polarization towards diverging perspectives, rather than convergence, when exposed to mixed evidence (Nickerson, 1998). Moreover, participants in the studies reviewed here rarely reversed their views (i.e., crossed the dividing line between guilt and innocence during their continuous ratings). Participants' initial appraisals may have been shaped by the representativeness heuristic, whereby judgments are guided by perceived similarity to familiar character types or narrative tropes (Tversky & Kahneman, 1974). These early impressions may then serve as anchors in ongoing evaluations, with new evidence insufficiently shifting participants away from their initial hypothesis, a process consistent with the anchoring and adjustment heuristic (Tversky & Kahneman, 1974). Even in the face of contradictory information, participants may have selectively integrated or discounted cues in a way that preserved coherence with their anchored belief, contributing to the increasingly divergent appraisals observed between interpretive clusters over time. While our data cannot definitively establish the use of these heuristics, such mechanisms offer a plausible cognitive account of how individuals form and sustain interpretive commitments during naturalistic decision-making under uncertainty. This pattern aligns with findings from my previously-noted study in which simple heuristic-like perspective assignments (e.g., friend of the victim vs. friend of the accused) shaped both initial certainty and the interpretation of ambiguous evidence (Mitchell et al., In Preparation). Even when exposed to identical stimuli, participants interpreted uncertainty-resolving information in perspective-consistent ways, suggesting that prior beliefs can bias not only initial expectations but also the perceived informativeness of subsequent cues.

Although participants did not directly interact, the emergence of appraisal synchrony within a socially framed context, potentially shaped by confirmation biases and heuristic processing, may offer insight into collective dynamics underlying echo chambers (Garrett, 2009) and the formation of conspiratorial beliefs (Douglas et al., 2017).

Shared Reality and Mentalizing

Our findings may also speak to broader questions in the social neuroscience of shared reality and mentalizing. Shared reality theory posits that individuals strive to achieve common internal representations of the world with others, particularly in ambiguous or uncertain contexts, as a means of fostering social connection and epistemic confidence (Echterhoff et al., 2009). The observed appraisal synchrony among participants who initially shared interpretive perspectives suggests that shared mental states may not arise solely through direct communication or social interaction, but can emerge passively through common interpretive frames applied to the same ambiguous stimulus. This aligns with evidence from naturalistic neuroimaging studies showing that shared prior beliefs can enhance neural synchrony and facilitate convergent interpretation (Nguyen et al., 2019; Yeshurun et al., 2017).

Moreover, the brain regions identified in our analyses, particularly those in the default mode and salience networks, are frequently implicated in mentalizing, or the attribution of mental states to others (Frith & Frith, 2012; Schilbach et al., 2008). The modulation of these regions by both interpretive alignment and stimulus complexity suggests that mentalizing processes may not be limited to explicit social cognition, but may also support the construction of shared understanding during socially framed, uncertain experiences. These results support the view that shared reality and mentalizing are dynamically co-constructed, with initial appraisals potentially guiding attention, belief updating, and the perceived informativeness of evidence in socially meaningful ways.

Interpreting Neural Findings in Naturalistic Contexts

Our findings largely align with and extend prior trial-based investigations of social and non-social uncertainty. We observed that social appraisals of uncertainty were reliably associated with activity in the lateral PFC, insulae, and precuneus, after adjusting for stimulus complexity. In contrast, non-social uncertainty was more strongly supported by the intraparietal sulcus (IPS) and sensory cortices. Social analyses also yielded relationships in regions commonly associated with social cognition, such as bilateral temporal poles, the dorsal PFC, and posterior cingulate cortex, which may constitute part of social decision-making circuitry (Frith & Frith, 2006, 2012).

The use of dynamic, naturalistic narratives in conjunction with synchrony-based analytic techniques may account for the engagement of brain regions not commonly implicated in trial-based studies of uncertainty. In particular, regions such as the parahippocampal cortex (PHC), parieto-occipital cortex (POC), and superior parietal lobe (SPL) may become especially relevant in the context of rich, temporally unfolding narratives that require social interpretation over time. The PHC, for example, has long been associated with contextual integration, supporting episodic memory by binding “who, what, when, and where” information (M. Li et al., 2016), and facilitating theory of mind via scene construction and mental simulation (Blomkvist, 2025). Its recruitment during naturalistic tasks may reflect the need to encode and retrieve the broader spatiotemporal setting in which social events unfold, particularly when those events must be interpreted through the lens of character motivations and shifting narrative context (Aminoff et al., 2007; Bar, 2004). Functional connectivity between the PHC and default mode network hubs such as the medial prefrontal cortex and posterior cingulate cortex may further enable contextual information to scaffold abstract social appraisals (Ward et al., 2014).

Similarly, the POC may contribute to naturalistic appraisals by integrating lower-level perceptual information with higher-order inferential processes. Prior work has shown that POC synchrony increases when subjects converge in attentional focus and mental state inference during complex video viewing (Bacha-Trams et al., 2017), consistent with its proposed role in autobiographical memory retrieval and scene modeling (Jääskeläinen & Kosonogov, 2023). The SPL may also be more prominently engaged in naturalistic settings due to its role in top-down attentional control, supporting flexible reorientation to socially salient cues, shifting goals, and emotionally charged events as they unfold (Corbetta & Shulman, 2002; Jääskeläinen & Kosonogov, 2023). The SPL also represented one of the few regions that synchronized across both social and non-social domains, which may represent the unique cognitive demands that resolving uncertainty begs in complex settings, regardless of domain. Together, these regions may be preferentially recruited in paradigms that more closely approximate real-world social cognition, capturing the interpretive demands and ambiguity inherent in everyday appraisal.

Limitations

Several methodological and conceptual limitations should be noted. First, my protocol to set video volumes to subject preferences, especially in the noisy MRI environment, meant that subjects occasionally requested volume changes mid-experiment. While participants were permitted to request volume adjustments between runs, I did not systematically document the timing or magnitude of these changes. This variability in auditory presentation may have introduced noise, particularly in language or temporally sensitive regions such as the superior temporal sulcus or auditory cortex. Although intersubject correlation (ISC) techniques emphasize shared temporal dynamics rather than signal magnitude, and random intercepts were modeled at the run level to absorb potential nuisance variance in hierarchical linear models, future studies should more rigorously control and log these factors.

Second, numerous analytic decisions were made (i.e., researcher degrees of freedom) that may be fundamentally arbitrary. Parameters for the sliding window analyses - including window size, step size, and sigma value - were chosen based on theoretical rationale and prior studies, but alternative parameterizations may yield different results. An additional example includes the assumption that participants' certainty ratings followed a bipolar construct (i.e., certainty of guilt vs. certainty of innocence), which may have led to an overemphasis on valence directionality. It is possible that many brain regions instead respond to fluctuations in certainty regardless of valence. I also employed a specific spatial resolution (e.g., 100-parcel Schaefer atlas), but other parcellation schemes or more fine-grained ROI definitions might have yielded different patterns of synchrony or cluster structure.

Third, my sample size was modest, and further subdivided due to experimental manipulations (e.g., rating vs. passive conditions; divergent interpretive perspectives), which limits statistical power and generalizability. Although random effects structures and mixed-effects models were used to partially mitigate this, replication in larger, more demographically diverse samples is necessary to validate and extend the present findings.

Fourth, although I implemented a luminance-based rating condition to serve as a non-social control, I did not include an alternative social appraisal control condition that was less epistemically focused (e.g., judgments of warmth or attractiveness). As a result, it is difficult to determine whether observed differences in synchrony and complexity were specific to certainty processing or social appraisal more broadly. This non-social control also differed from the social task considerably in length of time and rating variability, both of which may have had downstream effects on my ability to detect statistical effects.

Fifth, while intersubject synchrony is used to index convergence in interpretation or appraisal, converging synchrony does not uniquely indicate interpretive alignment. It may also reflect shared attention, arousal, or stimulus features. This ambiguity limits the specificity of the neural-behavioral mapping.

Sixth, the study relied on a single audiovisual narrative stimulus centered on a legal drama involving criminal guilt. This context may not generalize to other forms of social uncertainty (e.g., trust, moral conflict, or cooperation). Guilt certainty is a particularly specific operationalization of social cognition and may recruit distinct neural mechanisms not representative of other interpretive processes. Relatedly, the manipulation in the appraisal framing study was unidirectional (i.e., participants were given reasons to believe in guilt, but no conditions framed the target character as plausibly innocent). This asymmetry limits my ability to infer how positive evidence or exonerating details would influence appraisal dynamics.

Additionally, subjects in the appraisal manipulating study provided evidence to suggest that my manipulation was not fully successful. When asked "Based on what you saw, do you believe [Character] is guilty of the murder?", approximately 34% of subjects (i.e., 8 out of 23) indicated that they did not. These suspicious participants were relatively well-distributed among the characters (Jonathan: 40%, Grace: 17%, Franklin: 33%, Fernando: 50%) and 75% of them indicated that they grew less certain of the character's guilt over time. This mirrors an issue encountered in Mitchell et al. (In Preparation) in which some roles were consistently more difficult for subjects to adopt than others. Future studies should pilot role adaptability beforehand.

Finally, despite strong theoretical justification for continuous, in-the-moment ratings, it remains unclear how closely these ratings reflect real-time internal states versus reflective judgments influenced by metacognitive awareness. While this approach improves ecological validity, future work should further validate how well such expressive engagement captures underlying cognitive-affective processes.

Future Directions

There are at least a few ways in which the work outlined here can be built upon. First, a comprehensive multiverse analysis was originally planned to evaluate the robustness of my findings across a wide range of analytic decisions. Although the primary analyses were conducted using a 60s window, 12s step size, $\sigma = 3$, the 100-parcel Schaefer atlas, and raw appraisal values, I also generated parallel models using alternative specifications, including 40s and 80s windows, step sizes of 6s and 18s, σ values of 1 and 10, a 400-parcel resolution, and absolute-valued appraisals. These design choices yield 432 possible analytical permutations. While results have been computed, they could not be fully interpreted in time for this dissertation; however, they will be incorporated into forthcoming manuscripts to characterize the stability and generalizability of the observed effects.

Second, this dissertation did not leverage the full potential of the rich free recall data acquired from participants after stimulus viewing. These narratives offer a window into individual differences in memory, attention, and appraisals, and may provide a critical interpretive bridge between behavioral clustering and neural synchrony findings. Future analyses will aim to extract structured information from these narratives, with particular attention to how participants prioritize, sequence, and emotionally frame key events.

Finally, a follow-up fMRI study is currently underway that directly addresses several limitations of the initial appraisal experiment. In this new design, the stimulus is divided into four equally timed (~11 min) segments, and each participant completes one of four tasks per segment: passive viewing, social appraisal (guilt certainty), non-social appraisal (luminance), or a novel social judgment task (Jonathan's likeability). This structure ensures equivalent exposure across tasks and introduces a more ecologically valid social control condition. Additional improvements include an expanded sample size ($N = 60$), improved sound calibration, and the inclusion of a behavioral risk/uncertainty task (i.e., Iowa Gambling Task) for half the sample to explore how general uncertainty sensitivity relates to the dynamics of social appraisal. Together, these future efforts will significantly deepen and refine our understanding of how people resolve uncertainty in complex, socially relevant contexts.

Conclusions

In this dissertation, I examined how individuals appraise uncertainty in complex, dynamic circumstances, demonstrating that consensus in appraisals is shaped not only by moment-to-moment neural synchrony, but also by domain-specific context, perspective, and stimulus complexity. By leveraging continuous behavioral reports and intersubject neural analyses during video stimuli, I highlighted patterns of appraisal alignment, neural correlates of shared interpretation, and task-general circuitry supporting uncertainty resolution. These findings suggest that under ambiguity, social cognition is scaffolded by both shared neural architecture and interpretive priors that bias the appraisal process. Critically, regions traditionally underrepresented in trial-based paradigms emerged as central hubs in navigating naturalistic uncertainty, underscoring the value of ecologically valid methods. While this work cannot sufficiently establish mechanisms underlying the observed patterns of diverging certainty trajectories, it offer a window into the psychological and neural phenomena driving complex interpretations over time.

REFERENCES

Allen, E. A., Damaraju, E., Plis, S. M., Erhardt, E. B., Eichele, T., & Calhoun, V. D. (2014). Tracking Whole-Brain Connectivity Dynamics in the Resting State. *Cerebral Cortex*, *24*(3), 663–676. https://doi.org/10.1093/cercor/bhs352

Alós-Ferrer, C., & Farolfi, F. (2019). Trust Games and Beyond. *Frontiers in Neuroscience*, *13*, 887. https://doi.org/10.3389/fnins.2019.00887

Alós-Ferrer, C., Granić, Đ.-G., Shi, F., & Wagner, A. K. (2012). Choices and preferences: Evidence from implicit choices and response times. *Journal of Experimental Social Psychology*, *48*(6), 1336–1342. psyh. https://doi.org/10.1016/j.jesp.2012.07.004

Aminoff, E., Gronau, N., & Bar, M. (2007). The parahippocampal cortex mediates spatial and nonspatial associations. *Cerebral Cortex (New York, N.Y.: 1991)*, *17*(7), 1493–1503. https://doi.org/10.1093/cercor/bhl078

Andric, M., Goldin-Meadow, S., Small, S. L., & Hasson, U. (2016). Repeated movie viewings produce similar local activity patterns but different network configurations. *NeuroImage*, *142*, 613–627. https://doi.org/10.1016/j.neuroimage.2016.07.061

Antony, J. W., Hartshorne, T. H., Pomeroy, K., Gureckis, T. M., Hasson, U., McDougle, S. D., & Norman, K. A. (2021). Behavioral, Physiological, and Neural Signatures of Surprise during Naturalistic Sports Viewing. *Neuron*, *109*(2), 377-390.e7. https://doi.org/10.1016/j.neuron.2020.10.029

Avants, B. B., Epstein, C. L., Grossman, M., & Gee, J. C. (2008). Symmetric diffeomorphic image registration with cross-correlation: Evaluating automated labeling of elderly and neurodegenerative brain. *Medical Image Analysis*, *12*(1), 26–41. https://doi.org/10.1016/j.media.2007.06.004

Bacha-Trams, M., Glerean, E., Dunbar, R., Lahnakoski, J. M., Ryyppö, E., Sams, M., & Jääskeläinen, I. P. (2017). Differential inter-subject correlation of brain activity when kinship is a variable in moral dilemma. *Scientific Reports*, *7*(1). https://doi.org/10.1038/s41598-017-14323-x

Baldassano, C., Chen, J., Zadbood, A., Pillow, J. W., Hasson, U., & Norman, K. A. (2017). Discovering Event Structure in Continuous Narrative Perception and Memory. *Neuron*, *95*(3), 709-721.e5. https://doi.org/10.1016/j.neuron.2017.06.041

Bar, M. (2004). Visual objects in context. *Nature Reviews Neuroscience*, *5*(8), 617–629. https://doi.org/10.1038/nrn1476

Bates, D., Maechler, M., Bolker, B., & Walker, S. (2015). Fitting Linear Mixed-Effects Models Using lme4. *Journal of Statistical Software*, *67*(1), 1–48. https://doi.org/10.18637/jss.v067.i01

Behzadi, Y., Restom, K., Liau, J., & Liu, T. T. (2007). A component based noise correction method (CompCor) for BOLD and perfusion based fMRI. *NeuroImage*, *37*(1), 90–101. https://doi.org/10.1016/j.neuroimage.2007.04.042

Birrell, J., Meares, K., Wilkinson, A., & Freeston, M. (2011). Toward a definition of intolerance of uncertainty: A review of factor analytical studies of the Intolerance of Uncertainty Scale. *Clinical Psychology Review*, *31*(7), 1198–1208. https://doi.org/10.1016/j.cpr.2011.07.009

Blankenstein, N. E., Crone, E. A., van den Bos, W., & van Duijvenvoorde, A. C. K. (2016). Dealing With Uncertainty: Testing Risk- and Ambiguity-Attitude Across Adolescence. *Developmental Neuropsychology*, *41*(1–2), 77–92. https://doi.org/10.1080/87565641.2016.1158265

Blomkvist, A. (2025). Shaping the Space: A Role for the Hippocampus in Mental Imagery Formation. *Vision*, *9*(1), Article 1. https://doi.org/10.3390/vision9010002

Borja Jimenez, K. C., Abdelgabar, A. R., De Angelis, L., McKay, L. S., Keysers, C., & Gazzola, V. (2020). Changes in brain activity following the voluntary control of empathy. *NeuroImage*, *216*, 116529. https://doi.org/10.1016/j.neuroimage.2020.116529

Brudner, E. G., Karousatos, A. J., Fareri, D. S., & Delgado, M. R. (2021). Trust and Reputation: How Knowledge about Others Shapes Our Decisions. In F. Krueger (Ed.), *The Neurobiology of Trust* (pp. 155–184). Cambridge University Press; Cambridge Core. https://doi.org/10.1017/9781108770880.010

Carleton, R. N., Mulvogue, M. K., Thibodeau, M. A., McCabe, R. E., Antony, M. M., & Asmundson, G. J. G. (2012). Increasingly certain about uncertainty: Intolerance of uncertainty across anxiety and depression. *Journal of Anxiety Disorders*, *26*(3), 468–479. https://doi.org/10.1016/j.janxdis.2012.01.011

Chaiken, S., & Ledgerwood, A. (2012). A theory of heuristic and systematic information processing. In *Handbook of theories of social psychology, Vol. 1* (pp. 246–266). Sage Publications Ltd. https://doi.org/10.4135/9781446249215.n13

Chang, L., Eshin Jolly, Cheong, J. H., Burnashev, A., & Chen, A. (2018). *cosanlab/nltools: 0.3.11* [Computer software]. Zenodo. https://doi.org/10.5281/ZENODO.2229813

Chen, J., Leong, Y. C., Honey, C. J., Yong, C. H., Norman, K. A., & Hasson, U. (2017). Shared memories reveal shared structure in neural activity across individuals. *Nature Neuroscience*, *20*(1), 115–125. https://doi.org/10.1038/nn.4450

Chu, V. C., Lucas, G. M., Lei, S., Mozgai, S., Khooshabeh, P., & Gratch, J. (2019). Emotion regulation in the prisoner's dilemma: Effects of reappraisal on behavioral measures and cardiovascular measures of challenge and threat. *Frontiers in Human Neuroscience*, *13*. psyh. https://doi.org/10.3389/fnhum.2019.00050

Clark, U. S., Miller, E. R., & Hegde, R. R. (2018). Experiences of Discrimination Are Associated With Greater Resting Amygdala Activity and Functional Connectivity. *Biological Psychiatry: Cognitive Neuroscience and Neuroimaging*, *3*(4), 367–378. https://doi.org/10.1016/j.bpsc.2017.11.011

Corbetta, M., & Shulman, G. L. (2002). Control of goal-directed and stimulus-driven attention in the brain. *Nature Reviews. Neuroscience*, *3*(3), 201–215. https://doi.org/10.1038/nrn755

Cox, R. W., & Hyde, J. S. (1997). Software tools for analysis and visualization of fMRI data. *NMR in Biomedicine*, *10*(4–5), 171–178. https://doi.org/10.1002/(sici)1099-1492(199706/08)10:4/5<171::aid-nbm453>3.0.co;2-l

de la Vega, A., Rocca, R., Blair, R. W., Markiewicz, C. J., Mentch, J., Kent, J. D., Herholz, P., Ghosh, S. S., Poldrack, R. A., & Yarkoni, T. (2022). Neuroscout, a unified platform for generalizable and reproducible fMRI research. *bioRxiv*. https://doi.org/10.1101/2022.04.05.487222

De Leeuw, J. R., Gilbert, R. A., & Luchterhandt, B. (2023). jsPsych: Enabling an Open-Source CollaborativeEcosystem of Behavioral Experiments. *Journal of Open Source Software*, *8*(85), 5351. https://doi.org/10.21105/joss.05351

Delgado, M. R., Frank, R. H., & Phelps, E. A. (2005). Perceptions of moral character modulate the neural systems of reward during the trust game. *Nature Neuroscience*, *8*(11), 1611–1618. https://doi.org/10.1038/nn1575

Deutsch, M. (1960). The Effect of Motivational Orientation upon Trust and Suspicion. *Human Relations*, *13*(2), 123–139. https://doi.org/10.1177/001872676001300202

Douglas, K. M., Sutton, R. M., & Cichocka, A. (2017). The Psychology of Conspiracy Theories. *Current Directions in Psychological Science*, *26*(6), 538–542. https://doi.org/10.1177/0963721417718261

Dovidio, J. F., & Gaertner, S. L. (2000). Aversive Racism and Selection Decisions: 1989 and 1999. *Psychological Science*, *11*(4), 315–319. https://doi.org/10.1111/1467-9280.00262

DuPre, E., Hanke, M., & Poline, J.-B. (2020). Nature abhors a paywall: How open science can realize the potential of naturalistic stimuli. *NeuroImage*, *216*, 116330. https://doi.org/10.1016/j.neuroimage.2019.116330

Dwivedi, V. D., Goertz, K. E., & Selvanayagam, J. (2018). Heuristics in Language Comprehension. *Journal of Behavioral and Brain Science*, *8*(7), Article 7. https://doi.org/10.4236/jbbs.2018.87027

Echterhoff, G., Higgins, E. T., & Levine, J. M. (2009). Shared Reality: Experiencing Commonality with others' Inner States about the World. *Perspectives on Psychological Science*, *4*(5), 496–521. https://doi.org/10.1111/j.1745-6924.2009.01161.x

Ellsberg, D. (1961). Risk, Ambiguity, and the Savage Axioms. *Quarterly Journal of Economics*, *75*(27), 27. https://doi.org/10.2307/1884324

Esteban, O., Blair, R., Markiewicz, C. J., Berleant, S. L., Moodie, C., Ma, F., Isik, A. I., Erramuzpe, A., Goncalves, M., Poldrack, R. A., & Gorgolewski, K. J. (2017). *Poldracklab/Fmriprep: 1.0.0-Rc5* [Computer software]. Zenodo. https://doi.org/10.5281/ZENODO.996169

Esteban, O., Markiewicz, C. J., Blair, R. W., Moodie, C. A., Isik, A. I., Erramuzpe, A., Kent, J. D., Goncalves, M., DuPre, E., Snyder, M., Oya, H., Ghosh, S. S., Wright, J., Durnez, J., Poldrack, R. A., & Gorgolewski, K. J. (2019). fMRIPrep: A robust preprocessing pipeline for functional MRI. *Nature Methods*, *16*(1), 111–116. https://doi.org/10.1038/s41592-018-0235-4

Fairley, K., Vyrastekova, J., Weitzel, U., & Sanfey, A. G. (2022). Beyond lottery-evoked ambiguity aversion: The neural signature of the types and the sources of uncertainty. *NeuroImage*, *251*, 119007. https://doi.org/10.1016/j.neuroimage.2022.119007

Fareri, D. S., & Delgado, M. R. (2014). Differential reward responses during competition against in- and out-of-network others. *Social Cognitive and Affective Neuroscience*, *9*(4), 412–420. https://doi.org/10.1093/scan/nst006

Fayn, K., Willemsen, S., Muralikrishnan, R., Manias, B. C., Menninghaus, W., & Schlotz, W. (2021). Full throttle: Demonstrating the speed, accuracy, and validity of a new method for continuous two-dimensional self-report and annotation. *Behavior Research Methods*, *53*(3), 1–15. https://doi.org/10.3758/s13428-021-01616-3

FeldmanHall, O., & Shenhav, A. (2019). Resolving uncertainty in a social world. *Nature Human Behaviour*, *3*(5), 426–435. https://doi.org/10.1038/s41562-019-0590-x

Fetzner, M. G., Horswill, S. C., Boelen, P. A., & Carleton, R. N. (2013). Intolerance of Uncertainty and PTSD Symptoms: Exploring the Construct Relationship in a Community Sample with a Heterogeneous Trauma History. *Cognitive Therapy and Research*, *37*(4), 725–734. https://doi.org/10.1007/s10608-013-9531-6

Finn, E. S., Corlett, P. R., Chen, G., Bandettini, P. A., & Constable, R. T. (2018). Trait paranoia shapes inter-subject synchrony in brain activity during an ambiguous social narrative. *Nature Communications*, *9*(1), 2043. https://doi.org/10.1038/s41467-018-04387-2

Fiske, S. T. (1992). Thinking is for doing: Portraits of social cognition from Daguerreotype to laserphoto. *Journal of Personality and Social Psychology*, *63*(6), 877–889. https://doi.org/10.1037/0022-3514.63.6.877

Fiske, S. T., Cuddy, A. J. C., & Glick, P. (2007). Universal dimensions of social cognition: Warmth and competence. *Trends in Cognitive Sciences*, *11*(2), 77–83. https://doi.org/10.1016/j.tics.2006.11.005

Folkman, S., & Lazarus, R. S. (1986). Stress processes and depressive symptomatology. *Journal of Abnormal Psychology*, *95*(2), 107–113. pdh. https://doi.org/10.1037/0021-843X.95.2.107

Fonov, V., Evans, A., McKinstry, R., Almli, C., & Collins, D. (2009). Unbiased nonlinear average age-appropriate brain templates from birth to adulthood. *NeuroImage*, *47*, S102. https://doi.org/10.1016/S1053-8119(09)70884-5

Fredrickson, B. L., & Kahneman, D. (1993). Duration Neglect in Retrospective Evaluations of Affective Episodes. *Journal of Personality and Social Psychology*, *65*(1), 45–55.

Friedman, N. P., & Gustavson, D. E. (2022). Do Rating and Task Measures of Control Abilities Assess the Same Thing? *Current Directions in Psychological Science*, *31*(3), 262–271. https://doi.org/10.1177/09637214221091824

Frith, C. D., & Frith, U. (2006). The Neural Basis of Mentalizing. *Neuron*, *50*(4), 531–534. https://doi.org/10.1016/j.neuron.2006.05.001

Frith, C. D., & Frith, U. (2012). Mechanisms of social cognition. *Annual Review of Psychology*, *63*, 287–313. https://doi.org/10.1146/annurev-psych-120710-100449

Fujino, J., Hirose, K., Tei, S., Kawada, R., Tsurumi, K., Matsukawa, N., Miyata, J., Sugihara, G., Yoshihara, Y., Ideno, T., Aso, T., Takemura, K., Fukuyama, H., Murai, T., & Takahashi, H. (2016). Ambiguity aversion in schizophrenia: An fMRI study of decision-making under risk and ambiguity. *Schizophrenia Research*, *178*(1–3), 94–101. https://doi.org/10.1016/j.schres.2016.09.006

Garrett, R. K. (2009). Echo chambers online?: Politically motivated selective exposure among Internet news users1. *Journal of Computer-Mediated Communication*, *14*(2), 265–285. https://doi.org/10.1111/j.1083-6101.2009.01440.x

Gershman, S. J., Horvitz, E. J., & Tenenbaum, J. B. (2015). Computational rationality: A converging paradigm for intelligence in brains, minds, and machines. *Science*, *349*(6245), 273–278. https://doi.org/10.1126/science.aac6076

Girard, J. M., & Wright, A. G. C. (2018). DARMA: Software for dual axis rating and media annotation. *Behavior Research Methods*, *50*(3), 902–909. https://doi.org/10.3758/s13428-017-0915-5

Goldberg, H., Preminger, S., & Malach, R. (2014). The emotion–action link? Naturalistic emotional stimuli preferentially activate the human dorsal visual stream. *NeuroImage*, *84*, 254–264. https://doi.org/10.1016/j.neuroimage.2013.08.032

Gorgolewski, K., Burns, C. D., Madison, C., Clark, D., Halchenko, Y. O., Waskom, M. L., & Ghosh, S. S. (2011). Nipype: A Flexible, Lightweight and Extensible Neuroimaging Data Processing Framework in Python. *Frontiers in Neuroinformatics*, *5*. https://doi.org/10.3389/fninf.2011.00013

Greve, D. N., & Fischl, B. (2009). Accurate and robust brain image alignment using boundary-based registration. *NeuroImage*, *48*(1), 63–72. https://doi.org/10.1016/j.neuroimage.2009.06.060

Gross, J. J., & Levenson, R. W. (1995). Emotion Elicitation Using Films. *Cognition & Emotion*, *9*(1), 87–108.

Halchenko, Y., Goncalves, M., Castello, M. V. di O., Ghosh, S., Salo, T., Hanke, M., Velasco, P., Dae, Kent, J., Brett, M., Amlien, I., Gorgolewski, C., Lukas, D. C., Markiewicz, C., Tilley, S., Kaczmarzyk, J., Stadler, J., Kim, S., Kahn, A., … Meyer, K. (2021). *Nipy/heudiconv:* (Version v0.10.0) [Computer software]. Zenodo. https://doi.org/10.5281/zenodo.5557588

Hari, R., Henriksson, L., Malinen, S., & Parkkonen, L. (2015). Centrality of Social Interaction in Human Brain Function. *Neuron*, *88*(1), 181–193. https://doi.org/10.1016/j.neuron.2015.09.022

Hasson, U., Furman, O., Clark, D., Dudai, Y., & Davachi, L. (2008). Enhanced Intersubject Correlations during Movie Viewing Correlate with Successful Episodic Encoding. *Neuron*, *57*(3), 452–462. https://doi.org/10.1016/j.neuron.2007.12.009

Hasson, U., Ghazanfar, A. A., Galantucci, B., Garrod, S., & Keysers, C. (2012). Brain-to-brain coupling: A mechanism for creating and sharing a social world. *Trends in Cognitive Sciences*, *16*(2), 114–121. https://doi.org/10.1016/j.tics.2011.12.007

Hasson, U., Landesman, O., Knappmeyer, B., Vallines, I., Rubin, N., & Heeger, D. J. (2008). Neurocinematics: The Neuroscience of Film. *Projections*, *2*(1), 1–26.

Hasson, U., Nir, Y., Levy, I., Fuhrmann, G., & Malach, R. (2004). Intersubject Synchronization of Cortical Activity During Natural Vision. *Science*, *303*(5664), 1634–1640. https://doi.org/10.1126/science.1089506

Hendriks, M. H. A., Daniels, N., Pegado, F., & Op de Beeck, H. P. (2017). The Effect of Spatial Smoothing on Representational Similarity in a Simple Motor Paradigm. *Frontiers in Neurology*, *8*, 222. https://doi.org/10.3389/fneur.2017.00222

Hertz, U., Tyropoulou, E., Traberg, C., & Bahrami, B. (2020). Self-competence increases the willingness to pay for social influence. *Scientific Reports*, *10*(1), 17813. https://doi.org/10.1038/s41598-020-74857-5

Heusser, A. C., Fitzpatrick, P. C., & Manning, J. R. (2021). Geometric models reveal behavioural and neural signatures of transforming experiences into memories. *Nature Human Behaviour*, *5*(7), 905–919. https://doi.org/10.1038/s41562-021-01051-6

Hutcherson, C. A., Goldin, P. R., Ochsner, K. N., Gabrieli, J. D. E., Barrett, L. F., & Gross, J. J. (2005). Attention and emotion: Does rating emotion alter neural responses to amusing and sad films? *NeuroImage*, *27*(3), 656–668. https://doi.org/10.1016/j.neuroimage.2005.04.028

IEEE Standard for Floating-Point Arithmetic. (2019). IEEE. https://doi.org/10.1109/IEEESTD.2019.8766229

Jääskeläinen, I. P., Iiro P. Jääskëlainen, Ahveninen, J., Jyrki Ahveninen, Vasily Klucharev, Vasily Klucharev, Anna N. Shestakova, Анна Шестакова, Levy, J., Levy, J. C., & Jonathan Lévy. (2022). Behavioral Experience-Sampling Methods in Neuroimaging Studies With Movie and Narrative Stimuli. *Frontiers in Human Neuroscience*, *16*. https://doi.org/10.3389/fnhum.2022.813684

Jääskeläinen, I. P., & Kosonogov, V. (2023). Perspective taking in the human brain: Complementary evidence from neuroimaging studies with media-based naturalistic stimuli and artificial controlled paradigms. *Frontiers in Human Neuroscience*, *17*. psyh. https://doi.org/10.3389/fnhum.2023.1051934

Jenkinson, M., Bannister, P., Brady, M., & Smith, S. (2002). Improved optimization for the robust and accurate linear registration and motion correction of brain images. *NeuroImage*, *17*(2), 825–841. https://doi.org/10.1016/s1053-8119(02)91132-8

Jenkinson, M., Beckmann, C. F., Behrens, T. E. J., Woolrich, M. W., & Smith, S. M. (2012). FSL. *NeuroImage*, *62*(2), 782–790. https://doi.org/10.1016/j.neuroimage.2011.09.015

Jenkinson, M., & Smith, S. (2001). A global optimisation method for robust affine registration of brain images. *Medical Image Analysis*, *5*(2), 143–156. https://doi.org/10.1016/s1361-8415(01)00036-6

Jeremy Peterman, & Peterman, J. N. (1940). The “program analyzer”: A new technique in studying liked and disliked items in radio programs. *Journal of Applied Psychology*, *24*(6), 728–741. https://doi.org/10.1037/h0056834

Jern, A., Chang, K. K., & Kemp, C. (2014). Belief polarization is not always irrational. *Psychological Review*, *121*(2), 206–224. https://doi.org/10.1037/a0035941

Kagan, J. (1972). Motives and development. *Journal of Personality and Social Psychology*, *22*(1), 51–66. https://doi.org/10.1037/h0032356

Kahneman, D., & Tversky', A. (1978). Prospect Theory: An Analysis of Decision under Risk. *Econometrica*, *47*(2), 263–292.

Kassambara, A., & Mundt, F. (2020). *factoextra: Extract and Visualize the Results of Multivariate Data Analyses* (Version 1.0.7) [Computer software]. https://cran.r-project.org/web/packages/factoextra/index.html

Kimberley, T. J., Birkholz, D. D., Hancock, R. A., VonBank, S. M., & Werth, T. N. (2008). Reliability of fMRI during a Continuous Motor Task: Assessment of Analysis Techniques. *Journal of Neuroimaging*, *18*(1), 18–27. https://doi.org/10.1111/j.1552-6569.2007.00163.x

Kinreich, S., Djalovski, A., Kraus, L., Louzoun, Y., & Feldman, R. (2017). Brain-to-Brain Synchrony during Naturalistic Social Interactions. *Scientific Reports*, *7*(1), 17060. https://doi.org/10.1038/s41598-017-17339-5

Kragel, P. A., Reddan, M. C., LaBar, K. S., & Wager, T. D. (2019). Emotion schemas are embedded in the human visual system. *Science Advances*, *5*(7), eaaw4358. https://doi.org/10.1126/sciadv.aaw4358

Kriegeskorte, N., Mur, M., & Bandettini, P. (2008). Representational similarity analysis—Connecting the branches of systems neuroscience. *Frontiers in Systems Neuroscience*, *2*, 1–28. https://doi.org/10.3389/neuro.06.004.2008

Lahnakoski, J. M., Glerean, E., Jääskeläinen, I. P., Hyönä, J., Hari, R., Sams, M., & Nummenmaa, L. (2014). Synchronous brain activity across individuals underlies shared psychological perspectives. *NeuroImage*, *100*(100), 316–324. https://doi.org/10.1016/j.neuroimage.2014.06.022

Lanczos, C. (1964). Evaluation of Noisy Data. *Journal of the Society for Industrial and Applied Mathematics Series B Numerical Analysis*, *1*(1), 76–85. https://doi.org/10.1137/0701007

Lauharatanahirun, N., Aimone, J. A., & Gately, J. (2021). Behind the Veil of Ambiguity: Decision-Making under Social and Non-Social Sources of Uncertainty. *SSRN Electronic Journal*. https://doi.org/10.2139/ssrn.3937388

Levenson, R. W., & Gottman, J. M. (1983). Marital interaction: Physiological linkage and affective exchange. *Journal of Personality and Social Psychology*, *45*(3), 587–597. https://doi.org/10.1037/0022-3514.45.3.587

Levy, J., Lankinen, K., Hakonen, M., & Feldman, R. (2021). The integration of social and neural synchrony: A case for ecologically valid research using MEG neuroimaging. *Social Cognitive and Affective Neuroscience*, *16*(1–2), 143–152. https://doi.org/10.1093/scan/nsaa061

Li, F., Xie, R., Li, X., & Li, W. (2015). The influence of perceptual information on control processes involved in self-regulated learning: Evidence from item selection. *Psychonomic Bulletin & Review*, *22*(4), 1007–1013. https://doi.org/10.3758/s13423-014-0762-7

Li, M., Lu, S., & Zhong, N. (2016). The Parahippocampal Cortex Mediates Contextual Associative Memory: Evidence from an fMRI Study. *BioMed Research International*, *2016*, 9860604. https://doi.org/10.1155/2016/9860604

Li, R., Brannon, E. M., & Huettel, S. A. (2015). Children do not exhibit ambiguity aversion despite intact familiarity bias. *Frontiers in Psychology*, *5*. https://doi.org/10.3389/fpsyg.2014.01519

Li, X., Zhu, Y., Vuoriainen, E., Ye, C., & Astikainen, P. (2021). Decreased intersubject synchrony in dynamic valence ratings of sad movie contents in dysphoric individuals. *Scientific Reports*, *11*(1), 14419. https://doi.org/10.1038/s41598-021-93825-1

Liberty S. Hamilton, Hamilton, L. S., Alexander G. Huth, & Huth, A. G. (2020). The revolution will not be controlled: Natural stimuli in speech neuroscience. *Language, Cognition and Neuroscience*, *35*(5), 573–582. https://doi.org/10.1080/23273798.2018.1499946

Lieberman, M. D., Eisenberger, N. I., Crockett, M. J., Tom, S. M., Pfeifer, J. H., & Way, B. M. (2007). Putting Feelings Into Words Affect Labeling Disrupts Amygdala Activity in Response to Affective Stimuli. *Psychological Science*, *18*(5), 421–428. https://doi.org/10.1111/j.1467-9280.2007.01916.x

Lieberman, M. D., Inagaki, T. K., Tabibnia, G., & Crockett, M. J. (2011). Subjective responses to emotional stimuli during labeling, reappraisal, and distraction. *Emotion*, *11*(3), 468–480. pdh. https://doi.org/10.1037/a0023503

Lu, K., & Hao, N. (2019). When do we fall in neural synchrony with others? *Social Cognitive and Affective Neuroscience*, *14*(3), 253–261. https://doi.org/10.1093/scan/nsz012

Lyons, K. M., Stevenson, R. A., Owen, A. M., & Stojanoski, B. (2020). Examining the relationship between measures of autistic traits and neural synchrony during movies in children with and without autism. *NeuroImage: Clinical*, *28*, 102477. https://doi.org/10.1016/j.nicl.2020.102477

Ma, I., Westhoff, B., & van Duijvenvoorde, A. C. K. (2022). Uncertainty about others' trustworthiness increases during adolescence and guides social information sampling. *Scientific Reports*, *12*(1), 7634. https://doi.org/10.1038/s41598-022-09477-2

Martinez-Saito, M., & Gorina, E. (2022). Learning under social versus nonsocial uncertainty: A meta-analytic approach. *Human Brain Mapping*, *43*(13), 4185–4206. https://doi.org/10.1002/hbm.25948

Mauss, I. B., Levenson, R. W., McCarter, L., Wilhelm, F. H., & Gross, J. J. (2005). The tie that binds? Coherence among emotion experience, behavior, and physiology. *Emotion*, *5*(2), 175–190. https://doi.org/10.1037/1528-3542.5.2.175

Mauss, I. B., Shallcross, A. J., Troy, A. S., John, O. P., Ferrer, E., Wilhelm, F. H., & Gross, J. J. (2011). Don't hide your happiness! Positive emotion dissociation, social connectedness, and psychological functioning. *Journal of Personality and Social Psychology*, *100*(4), 738–748. https://doi.org/10.1037/a0022410

Mitchell, W. J. (2024). *Wj-mitchell/CoRVid.js* (Version v 0.1) [JavaScript]. https://github.com/wj-mitchell/CoRVid.js (Original work published 2024)

Mitchell, W. J., Schmidt, H., & Helion, C. (In Preparation). *Neural Effects of Continuous Ratings During Active Engagement Within a Video fMRI Paradigm*. https://doi.org/10.17605/OSF.IO/NHWA4

Mitchell, W. J., Stasiak, J., & Helion, C. (In Preparation). *Dynamic Moral Appraisal as a Function of Interpretive Perspective During Naturalistic Viewing*.

Mitchell, W. J., Tepfer, L. J., Henninger, N. M., Perlman, S. B., Murty, V. P., & Helion, C. (2021). Developmental Differences in Affective Representation Between Prefrontal and Subcortical Structures. *Social Cognitive and Affective Neuroscience*, *17*(3), 311–322. https://doi.org/10.1093/scan/nsab093

Morriss, J., Saldarini, F., & van Reekum, C. M. (2019). The role of threat level and intolerance of uncertainty in extinction. *International Journal of Psychophysiology*, *142*, 1–9. https://doi.org/10.1016/j.ijpsycho.2019.05.013

Nastase, S. A., Gazzola, V., Hasson, U., & Keysers, C. (2019). Measuring shared responses across subjects using intersubject correlation. *Social Cognitive and Affective Neuroscience*, 669–687. https://doi.org/10.1093/scan/nsz037

Nastase, S. A., Goldstein, A., & Hasson, U. (2020). Keep it real: Rethinking the primacy of experimental control in cognitive neuroscience. *NeuroImage*, *222*, 117254. https://doi.org/10.1016/j.neuroimage.2020.117254

Neys, W. D., Cromheeke, S., & Osman, M. (2011). Biased but in Doubt: Conflict and Decision Confidence. *PLOS ONE*, *6*(1), e15954. https://doi.org/10.1371/journal.pone.0015954

Nguyen, M., Vanderwal, T., & Hasson, U. (2019). Shared understanding of narratives is correlated with shared neural responses. *NeuroImage*, *184*, 161–170. https://doi.org/10.1016/j.neuroimage.2018.09.010

Nickerson, R. S. (1998). Confirmation Bias: A Ubiquitous Phenomenon in Many Guises. *Review of General Psychology*, *2*(2), 175–220. https://doi.org/10.1037/1089-2680.2.2.175

Nisbett, R. E., & Wilson, T. D. (1977). Telling more than we can know: Verbal reports on mental processes. *Psychological Review*, *84*(3), 231–259. https://doi.org/10.1037/0033-295X.84.3.231

Nummenmaa, L., Glerean, E., Viinikainen, M., Jääskeläinen, I. P., Hari, R., & Sams, M. (2012). Emotions promote social interaction by synchronizing brain activity across individuals. *Proceedings of the National Academy of Sciences of the United States of America*, *109*(24), 9599–9604. https://doi.org/10.1073/pnas.1206095109

Oglesby, M. E., Boffa, J. W., Short, N. A., Raines, A. M., & Schmidt, N. B. (2016). Intolerance of uncertainty as a predictor of post-traumatic stress symptoms following a traumatic event. *Fearing the Unknown*, *41*, 82–87. https://doi.org/10.1016/j.janxdis.2016.01.005

Pagliaccio, D., Kumar, P., Kamath, R. A., Pizzagalli, D. A., & Auerbach, R. P. (2022). Neural sensitivity to peer feedback and depression symptoms in adolescents: A 2-YEAR multiwave longitudinal study. *Journal of Child Psychology and Psychiatry*, jcpp.13690. https://doi.org/10.1111/jcpp.13690

Peirce, J., Gray, J. R., Simpson, S., MacAskill, M., Höchenberger, R., Sogo, H., Kastman, E., & Lindeløv, J. K. (2019). PsychoPy2: Experiments in behavior made easy. *Behavior Research Methods*, *51*(1), 195–203. https://doi.org/10.3758/s13428-018-01193-y

Popal, H. S., Wang, Y., & Olson, I. R. (2019). A Guide To Representational Similarity Analysis for Social Neuroscience. *Social Cognitive and Affective Neuroscience*, *14*(11), 1243–1253. https://doi.org/10.1093/scan/nsz099

Power, J. D., Mitra, A., Laumann, T. O., Snyder, A. Z., Schlaggar, B. L., & Petersen, S. E. (2014). Methods to detect, characterize, and remove motion artifact in resting state fMRI. *NeuroImage*, *84*, 320–341. https://doi.org/10.1016/j.neuroimage.2013.08.048

Poynton, C. (2003). *Digital video and HDTV algorithms and interfaces*. Morgan Kaufmann.

Qu, C., DeWind, N. K., & Brannon, E. M. (2022). Increasing entropy reduces perceived numerosity throughout the lifespan. *Cognition*, *225*, 105096. https://doi.org/10.1016/j.cognition.2022.105096

R Core Team. (2022). *R: A language and environment for statistical computing.* [Computer software]. R Foundation for Statistical Computing. https://www.R-project.org/

Ratcliff, R. (1978). A theory of memory retrieval. *Psychological Review*, *85*(2), 59–108. https://doi.org/10.1037/0033-295X.85.2.59

Ratcliff, R. (2002). A diffusion model account of response time and accuracy in a brightness discrimination task: Fitting real data and failing to fit fake but plausible data. *Psychonomic Bulletin & Review*, *9*(2), 278–291. https://doi.org/10.3758/BF03196283

Rousseeuw, P. J. (1987). Silhouettes: A graphical aid to the interpretation and validation of cluster analysis. *Journal of Computational and Applied Mathematics*, *20*, 53–65. https://doi.org/10.1016/0377-0427(87)90125-7

Ruef, A. M., & Levenson, R. W. (2007). Continuous Measurement of Emotion:The Affect Rating Dial. In J. A. Coan & J. J. B. Allen (Eds.), *Handbook of Emotion Elicitation and Assessment* (pp. 286–297). Oxford University PressNew York, NY. https://doi.org/10.1093/oso/9780195169157.003.0018

Saarimäki, H. (2021). Naturalistic Stimuli in Affective Neuroimaging: A Review. *Frontiers in Human Neuroscience*, *15*, 675068. https://doi.org/10.3389/fnhum.2021.675068

Satopaa, V., Albrecht, J., Irwin, D., & Raghavan, B. (2011). Finding a "Kneedle" in a Haystack: Detecting Knee Points in System Behavior. *2011 31st International Conference on Distributed Computing Systems Workshops*, 166–171. https://doi.org/10.1109/ICDCSW.2011.20

Satterthwaite, T. D., Elliott, M. A., Gerraty, R. T., Ruparel, K., Loughead, J., Calkins, M. E., Eickhoff, S. B., Hakonarson, H., Gur, R. C., Gur, R. E., & Wolf, D. H. (2013). An improved framework for confound regression and filtering for control of motion artifact in the preprocessing of resting-state functional connectivity data. *NeuroImage*, *64*, 240–256. https://doi.org/10.1016/j.neuroimage.2012.08.052

Schaefer, A., Kong, R., Gordon, E. M., Laumann, T. O., Zuo, X.-N., Holmes, A. J., Eickhoff, S. B., & Yeo, B. T. T. (2018). Local-Global Parcellation of the Human Cerebral Cortex from Intrinsic Functional Connectivity MRI. *Cerebral Cortex*, *28*(9), 3095–3114. https://doi.org/10.1093/cercor/bhx179

Schilbach, L., Eickhoff, S. B., Mojzisch, A., & Vogeley, K. (2008). What's in a smile? Neural correlates of facial embodiment during social interaction. *Social Neuroscience*, *3*(1), 37–50. https://doi.org/10.1080/17470910701563228

Shannon, C. E. (1948). A mathematical theory of communication. *The Bell System Technical Journal*, *27*(3), 379–423. https://doi.org/10.1002/j.1538-7305.1948.tb01338.x

Signorell, A., Aho, K., Alfons, A., Anderegg, N., Aragon, T., Arachchige, C., Arppe, A., Baddeley, A., Barton, K., Bolker, B., Borchers, H. W., Caeiro, F., Champely, S., Chessel, D., Chhay, L., Cooper, N., Cummins, C., Dewey, M., Doran, H. C., … Zeileis, A. (2025). *DescTools: Tools for Descriptive Statistics* (Version 0.99.60) [Computer software]. https://cran.r-project.org/web/packages/DescTools/index.html

Simony, E., & Chang, C. (2020). Analysis of stimulus-induced brain dynamics during naturalistic paradigms. *NeuroImage*, *216*, 116461. https://doi.org/10.1016/j.neuroimage.2019.116461

Smith, C. A., & Ellsworth, P. C. (1985). Patterns of cognitive appraisal in emotion. *Journal of Personality and Social Psychology*, *48*(4), 813–838. pdh. https://doi.org/10.1037/0022-3514.48.4.813

Song, H., Finn, E. S., & Rosenberg, M. D. (2021). Neural signatures of attentional engagement during narratives and its consequences for event memory. *Proceedings of the National Academy of Sciences*, *118*(33), e2021905118. https://doi.org/10.1073/pnas.2021905118

Sonkusare, S., Breakspear, M., & Guo, C. C. (2019). Naturalistic Stimuli in Neuroscience: Critically Acclaimed. *Trends in Cognitive Sciences*, *23*(8), 699–714. https://doi.org/10.1016/j.tics.2019.05.004

Stasiak, J. E., Mitchell, W. J., Reisman, S. S., Gregory, D. F., Murty, V. P., & Helion, C. (2023). Physiological arousal guides situational appraisals and metacognitive recall for naturalistic experiences. *Neuropsychologia*, *180*, 108467. https://doi.org/10.1016/j.neuropsychologia.2023.108467

Strange, B. A., Duggins, A., Penny, W., Dolan, R. J., & Friston, K. J. (2005). Information theory, novelty and hippocampal responses: Unpredicted or unpredictable? *Neural Networks*, *18*(3), 225–230. https://doi.org/10.1016/j.neunet.2004.12.004

Sutter, M., Kocher, M. G., Glätzle-Rützler, D., & Trautmann, S. T. (2013). Impatience and Uncertainty: Experimental Decisions Predict Adolescents' Field Behavior. *American Economic Review*, *103*(1), 510–531. https://doi.org/10.1257/aer.103.1.510

Taylor, S. F., Phan, K. L., Decker, L. R., & Liberzon, I. (2003). Subjective rating of emotionally salient stimuli modulates neural activity. *NeuroImage*, *18*(3), 650–659. https://doi.org/10.1016/S1053-8119(02)00051-4

Torre, J. B., & Lieberman, M. D. (2018). Putting Feelings Into Words: Affect Labeling as Implicit Emotion Regulation. *Emotion Review*, *10*(2), 116–124. https://doi.org/10.1177/1754073917742706

Trautmann, S. T., Vieider, F. M., & Wakker, P. P. (2008). Causes of ambiguity aversion: Known versus unknown preferences. *Journal of Risk and Uncertainty*, *36*(3), 225–243. https://doi.org/10.1007/s11166-008-9038-9

Tuckey, M. R., & Brewer, N. (2003). The influence of schemas, stimulus ambiguity, and interview schedule on eyewitness memory over time. *Journal of Experimental Psychology: Applied*, *9*(2), 101–118. https://doi.org/10.1037/1076-898X.9.2.101

Tustison, N. J., Avants, B. B., Cook, P. A., Zheng, Y., Egan, A., Yushkevich, P. A., & Gee, J. C. (2010). N4ITK: Improved N3 bias correction. *IEEE Transactions on Medical Imaging*, *29*(6), 1310–1320. https://doi.org/10.1109/TMI.2010.2046908

Tversky, A., & Kahneman, D. (1974). Judgment under Uncertainty: Heuristics and Biases. *Science*, *185*(4157), 1124–1131. https://doi.org/10.1126/science.185.4157.1124

Tymula, A., Rosenberg Belmaker, L. A., Roy, A. K., Ruderman, L., Manson, K., Glimcher, P. W., & Levy, I. (2012). Adolescents' risk-taking behavior is driven by tolerance to ambiguity. *Proceedings of the National Academy of Sciences*, *109*(42), 17135–17140. https://doi.org/10.1073/pnas.1207144109

van Rossum, G. (1995). *Python tutorial* (Version Technical Report CS-R9526) [Python].

Vives, M.-L., & FeldmanHall, O. (2018). Tolerance to ambiguous uncertainty predicts prosocial behavior. *Nature Communications*, *9*(1), 2156. https://doi.org/10.1038/s41467-018-04631-9

Wagner, V., Scharinger, M., Knoop, C. A., & Menninghaus, W. (2020). Effects of continuous self-reporting on aesthetic evaluation and emotional responses. *Poetics*, *85*, 101497. https://doi.org/10.1016/j.poetic.2020.101497

Ward, A. M., Schultz, A. P., Huijbers, W., Van Dijk, K. R. A., Hedden, T., & Sperling, R. A. (2014). The parahippocampal gyrus links the default-mode cortical network with the medial temporal lobe memory system. *Human Brain Mapping*, *35*(3), 1061–1073. https://doi.org/10.1002/hbm.22234

Westermann, R., Spies, K., Stahl, G., & Hesse, F. (1996). Relative effectiveness and validity of mood induction procedures: A meta-analysis. *European Journal of Social Psychology*, *26*(1996), 557–580.

Wickham, H., Averick, M., Bryan, J., Chang, W., McGowan, L. D., François, R., Grolemund, G., Hayes, A., Henry, L., Hester, J., Kuhn, M., Pedersen, T. L., Miller, E., Bache, S. M., Müller, K., Ooms, J., Robinson, D., Seidel, D. P., Spinu, V., … Yutani, H. (2019). Welcome to the tidyverse. *Journal of Open Source Software*, *4*(43), 1686. https://doi.org/10.21105/joss.01686

Xu, L., Bolt, T., Nomi, J. S., Li, J., Zheng, X., Fu, M., Kendrick, K. M., Becker, B., & Uddin, L. Q. (2020). Inter-subject phase synchronization differentiates neural networks underlying physical pain empathy. *Social Cognitive and Affective Neuroscience*, *15*(2), 225–233. https://doi.org/10.1093/scan/nsaa025

Ybarra, O., Keller, M. C., Chan, E., Garcia, S. M., Sanchez-Burks, J., Morrison, K. R., & Baron, A. S. (2010). Being unpredictable: Friend or foe matters. *Social Psychological and Personality Science*, *1*(3), 259–267. https://doi.org/10.1177/1948550610370214

Yeshurun, Y., Swanson, S., Simony, E., Chen, J., Lazaridi, C., Honey, C. J., & Hasson, U. (2017). Same Story, Different Story: The Neural Representation of Interpretive Frameworks. *Psychological Science*, *28*(3), 307–319. https://doi.org/10.1177/0956797616682029

Zhang, Y., Mańdziuk, J., Quek, C. H., & Goh, B. W. (2017). Curvature-based method for determining the number of clusters. *Information Sciences*, *415–416*, 414–428. https://doi.org/10.1016/j.ins.2017.05.024

Zhu, H. (2023). *The psychophysics of entropy judgments for musical note sequences* [Brooklyn College of CUNY]. Crump Lab. https://www.crumplab.com/midi-entropy-judgment/

APPENDIX

Alternative Non-Social Task for fMRI Appraisal Expression Study. Five early participants (prior to finalizing the luminance task) completed an alternate non-social evaluation involving a synthetic video of a digital fishtank. A vertical red line bisected the screen, and participants rated their certainty as to which side currently contained more fish. The fish would dynamically enter the screen from either the left or right side, swim about somewhat stochastically, and exit periodically on either the left of right. The video did not contain sound. Ratings shifted toward the side perceived as having a greater number of fish and hovered near the midpoint when uncertain. This pilot task was ultimately discontinued to better align the perceptual structure of the non-social task with that of the primary stimulus.

Audio Delivery for fMRI Appraisal Expression Study. Audio for the experimental task was presented through OptoAcoustics OptoActive sound-canceling headphones. To ensure clear and audible audio during MRI scanning, I analyzed the noise frequencies generated by the MRI machine during imaging. I compared these frequencies with those in my audio stimuli and used Adobe's Premiere Pro to shift any competing audio frequencies to non-competing frequency bands and applying reasonable compression upon the entire audio time course. This adjustment preserved the integrity of the audio experience for the subjects while minimizing interference from MRI noise. Presentation volume was adjusted to a comfortable level for each participant based upon subject feedback during a training exercise which featured royalty-free city noises played at a median volume that matched the median volume of my stimulus. Subjects could request volume changes between runs as needed. The visual elements of the experimental setup were projected on an MRI-compatible, out-of-bore screen using a Hyperion Projector.

Stimulus Break Assignment Procedure for Sparsely Sampled Social Appraisal Study. To balance ecological validity with data density, I employed a semi-randomized, algorithmically constrained procedure to determine the 34 stimulus breakpoints at which participants would be prompted for social judgments. The full stimulus was first divided into 1,322 candidate pause points, excluding the initial 30 seconds to allow participants to settle into the narrative. This resolution matched the TR used in the neuroimaging study to facilitate cross-study comparisons.

Each subject's sampling profile was generated by partitioning the stimulus into 34 equally spaced temporal windows and randomly selecting one timestamp per window. This ensured uniform distribution of sampling across the episode. A 60-second minimum interval between breaks was enforced to reduce participant fatigue and preserve narrative coherence.

To avoid clustering and enhance coverage, the order of subject assignment was dynamically reordered after each sampling step to prioritize participants with later prior selections. This adaptive procedure promoted temporal dispersion of judgments across subjects. Additionally, to ensure uniform group-level coverage, global constraints were applied such that no candidate pause point appeared fewer than twice or more than three times across the dataset. Oversampled points were replaced with nearby under-sampled points while maintaining spacing and clustering constraints.

These sampling configurations were indexed by subject ID (e.g., DH-###) and dynamically linked via a pre-assigned break ID using a purpose-built Pavlovia integration tool (https://moryscarter.com/vespr/pavlovia.php). Upon study launch, each participant's unique break schedule was called via a break_ids.js script, enabling consistent, real-time delivery of personalized sampling protocols.

Tables

Index	Network	Region		Neural Sync. x Domain (β)	Neural Sync. in Non-Social (β)	Neural Sync. in Social (β)
11	Default (C)	Left	parahippocampal cortex	-0.176 **	0.143 ***	-0.017
18	Control (B)	Left	temporal	-0.177 **	0.067 .	-0.107 *
21	Sal / Ventral Attn (A)	Left	frontal medial	-0.180 **	0.137 ***	-0.009
24	Sal / Ventral Attn (A)	Left	superior parietal lobule	-0.184 **	0.094 **	-0.040
28	Dorsal Attention (A)	Left	inferior parietal lobule	-0.223 ***	0.144 ***	-0.060
37	Auditory	Left	temporal	-0.171 **	0.126 ***	0.000
38	SomatoMotor (A)	Left	-	-0.346 ***	0.202 ***	-0.077 .
39	SomatoMotor (A)	Left	-	-0.260 ***	0.114 ***	-0.117 **
40	SomatoMotor (B)	Left	insula	-0.208 **	0.066 .	-0.142 **
42	SomatoMotor (B)	Left	-	-0.193 **	0.060 .	-0.103 *
44	Visual (A)	Left	extrastriate cortex	-0.184 ***	0.108 ***	-0.012
50	Visual (C)	Left	striate	-0.174 **	0.056 .	-0.095 *
68	Control (B)	Right	lateral prefrontal cortex	0.169 **	-0.017	0.094 *
75	Sal / Ventral Attn (A)	Right	inferior parietal lobule	-0.161 **	0.027	-0.080 *
89	SomatoMotor (A)	Right	-	-0.243 ***	0.066 .	-0.087 *
98	Visual (B)	Right	striate	-0.151 **	0.106 ***	-0.043

*Significance Key: . $p < 0.1$ | * $p < 0.05$ | ** $p < 0.01$ | *** $p < 0.001$*

Table 2. Appraisal-Neural Synchrony Parcels Moderated by Domain 16 regions demonstrated a significant (adjusted $p < 0.01$) neural synchrony by domain interaction (reference: non-social). Values in the final three columns represent standardized betas in the primary model, and two subsequent post-hoc models specified to probe domain-specific effects, respectively. Few regions that significantly predicted social appraisal synchrony also predicted non-social appraisal synchrony, demonstrating domain-specificity. Negative beta estimates are colored red.

Index	Network	Region	Neural Sync. x Perspective in Social (β)
4	Default (B)	Left frontal pole	0.306 **
9	Default (B)	Left temporal	-0.376 ***
13	Language	Left inferior frontal gyrus	0.207 .
14	Language	Left temporal	-0.274 **
16	Control (A)	Left lateral prefrontal cortex	0.254 *
19	Control (C)	Left cingulate posterior	0.358 ***
27	Sal. / Ventral Attn (B)	Left lateral prefrontal cortex	0.284 *
37	Auditory	Left temporal	-0.378 ***
43	Visual (A)	Left extrastriate cortex	-0.216 .
44	Visual (A)	Left extrastriate cortex	-0.225 *
54	Default (A)	Right temporal pole	-0.241 *
64	Control (A)	Right intraparietal sulcus	0.247 *
65	Control (A)	Right lateral prefrontal cortex	0.409 ***
70	Control (C)	Right cingulate posterior	0.287 *
72	Control (C)	Right medial posterior prefront	0.393 ***
80	Sal. / Ventral Attn (B)	Right lateral prefrontal cortex	0.388 ***
81	Sal. / Ventral Attn (B)	Right temporal	-0.259 **
94	Visual (A)	Right extrastriate cortex	-0.288 **
96	Visual (A)	Right extrastriate cortex	-0.240 *

*Significance Key: . $p < 0.1$ | * $p < 0.05$ | ** $p < 0.01$ | *** $p < 0.001$*

Table 3. Social Appraisal-Neural Synchrony Parcels Moderated by Perspective 5 regions appear to demonstrate greater appraisal - neural synchrony associations when sharing perspectives and 5 regions appear to demonstrate reduced appraisal neural synchrony associations when sharing perspectives following our adjusted $p < 0.01$ standard. Values represent standardized betas. Negative beta estimates are colored red.

Index	Network	Region	Neural Sync. x Complexity (β)	Neural Sync. x Domain x Complexity (β)	Neural Sync. x Complexity in Non-Social (β)	Neural Sync. x Complexity in Social (β)
2	Default (A)	Left temporal pole	0.079 *	0.265 **	-0.039	0.211 ***
7	Default (B)	Left dorsal prefrontal cortex	0.064 .	0.172 **	0.017	0.146 **
10	Default (C)	Left dorsal prefrontal cortex	-0.022	0.206 **	-0.067	0.088
24	Sal. / Ventral Attn (A)	Left superior parietal lobule	0.027	0.199 **	-0.063	0.149 **
25	Sal. / Ventral Attn (B)	Left inferior parietal lobule	0.069 *	0.226 **	-0.013	0.195 ***
31	Dorsal Attention (A)	Left superior parietal lobule	0.107 ***	0.188 **	0.010	0.225 ***
49	Visual (C)	Left extrastriate cortex	-0.004	0.187 **	-0.089 *	0.086 .
50	Visual (C)	Left striate	0.043	0.184 **	-0.034	0.117 *
52	Default (A)	Right dorsal prefrontal cortex	0.086 *	0.194 **	-0.035	0.184 ***
56	Default (B)	Right dorsal prefrontal cortex	0.079 *	0.188 **	0.016	0.162 **
57	Default (B)	Right temporal pole	0.034	0.308 ***	-0.077	0.208 ***
58	Default (C)	Right parahippocampal cortex	0.066 .	0.205 **	-0.003	0.135 *
75	Sal. / Ventral Attn (A)	Right inferior parietal lobule	-0.044	0.188 **	-0.113 **	0.067
76	Sal. / Ventral Attn (A)	Right superior parietal lobule	0.025	0.199 **	-0.083 *	0.116 *
86	Auditory	Right superior temporal	0.043	0.199 **	-0.041	0.094 .
93	SomatoMotor (B)	Right -	-0.016	0.202 **	-0.095 *	0.046
95	Visual (A)	Right extrastriate cortex	0.120 ***	0.175 **	0.027	0.212 ***

*Significance Key: . p < 0.1 | * p < 0.05 | ** p < 0.01 | *** p < 0.001*

Table 4. Appraisal-Neural Synchrony Parcels Moderated by Complexity Relatively view regions appeared demonstrate sensitivity in the appraisal-neural synchrony relationship depending upon how complex the stimulus across domains. However, for several regions, the way that neural synchrony and complexity interact to shape appraisal synchrony appears to depend on whether the context is social or non-social. Synchrony in several higher-cognition regions appears to more strongly predict social appraisal synchrony as complexity changes. However, that same relationship weakens or is not significant in the non-social domain. Values represent standardized betas. Negative beta estimates are colored red.